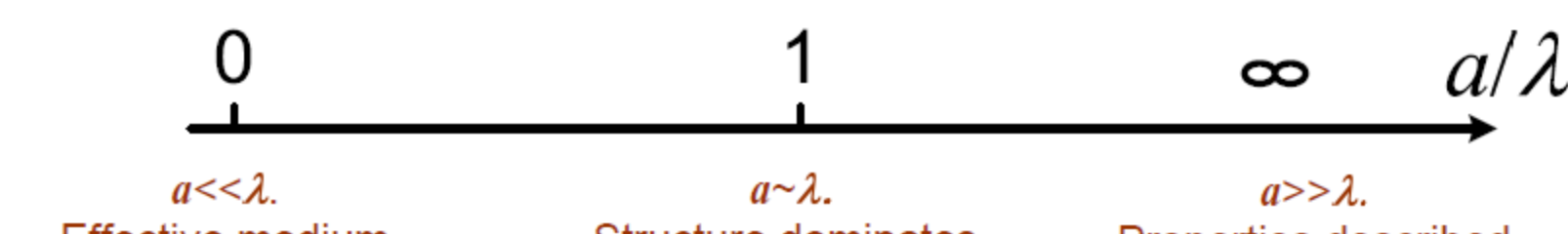
Photonic crystals. Metamaterials

http://ab-initio.mit.edu/photons/tutorial/

PH 673
Nanoscience and Nanotechnology
October 24, 2025

Electromagnetic properties v.s. characteristic sizes



Effective medium description using Maxwell equations with μ, ε, n, Z

Example:
Optical crystals
Metamaterials

Structure dominates.
Properties determined
by diffraction and
interference

Example:

Photonics crystals
Phased array radar
X-ray diffraction optics

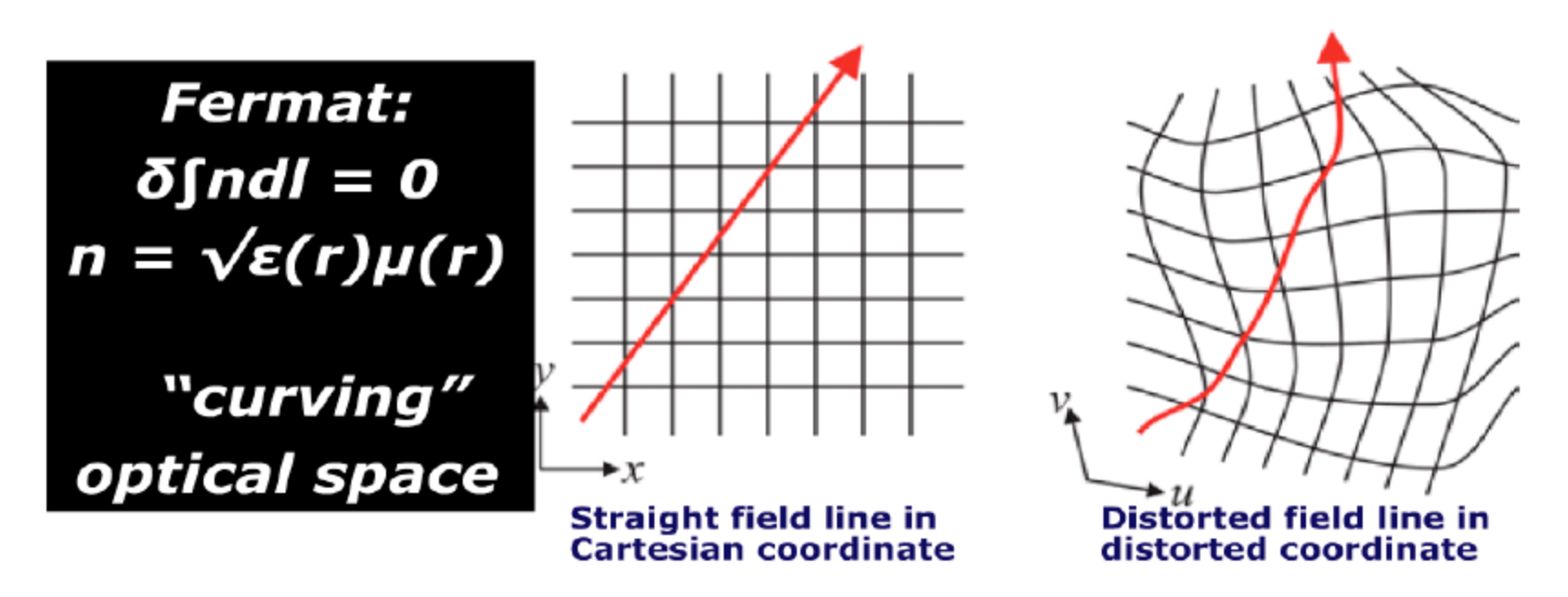
PC-"metamaterials" are not considered

Properties described using geometrical optics and ray tracing

Example: Lens system Shadows

Optical cloaking/invisibility

Designing space for light with transformation optics



Spatial profile of ϵ & μ tensors determines the distortion of coordinate

Seeking for profile of ϵ & μ to make light avoid particular region in space — optical cloaking

Pendry et al., Science, 2006

Introduction

C

A Photonic Crystal is a structure that has a periodic physical structure with a typical length scale on the order a wavelength

Periodicity leads to modified light propagation, reflection and diffraction

A Photonic Band Gap (PBG) material is a photonic crystal (1D, 2D or 3D) that has a sufficiently large index contrast to completely prevent propagation of light within a specific frequency range (band), leading to a gap in the dispersion relation

Applications:

- reflectors based on non-metallic materials (Bragg reflectors)
- strongly confined waveguides
- dispersion control (e.g. photonic bandgap fiber)
- laser cavities (1D, 2D or 3D)
- Single photon emission

Photonic crystals

Angle dependence can be modified by structuring in multiple directions:

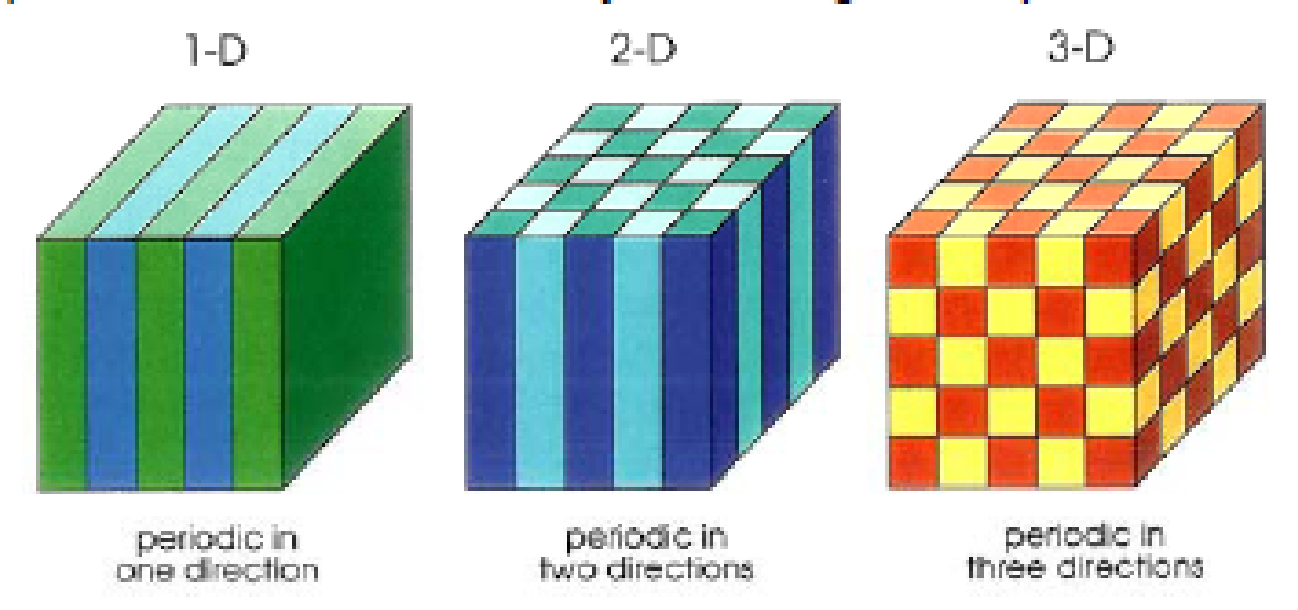


Figure 1 Simple examples of one-, two-, and three-dimensional photonic crystals. The different colors represent materials with different dielectric constants. The defining feature of a photonic crystal is the periodicity of dielectric material along one or more axes.

Easy to see: at normal incidence to any main axis, light undergoes periodic reflections ⇒ long range propagation not possible at certain angles

For high contrast: large gaps, angle requirement not so stringent: propagation forbidden in large overlapping angle ranges: complete 3D bandgap

Photonic Crystals- Semiconductors of Light

Semiconductors

Periodic array of atoms



Atomic length scales

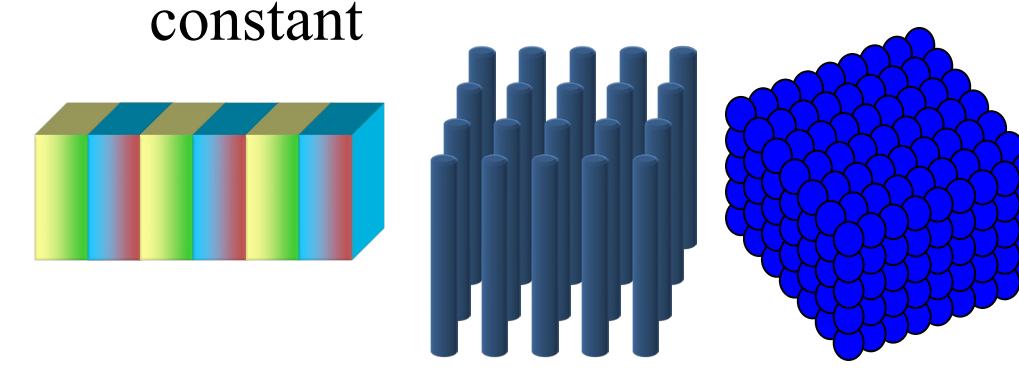
Natural structures

Control electron flow

1950's electronic revolution

Photonic Crystals

Periodic variation of dielectric

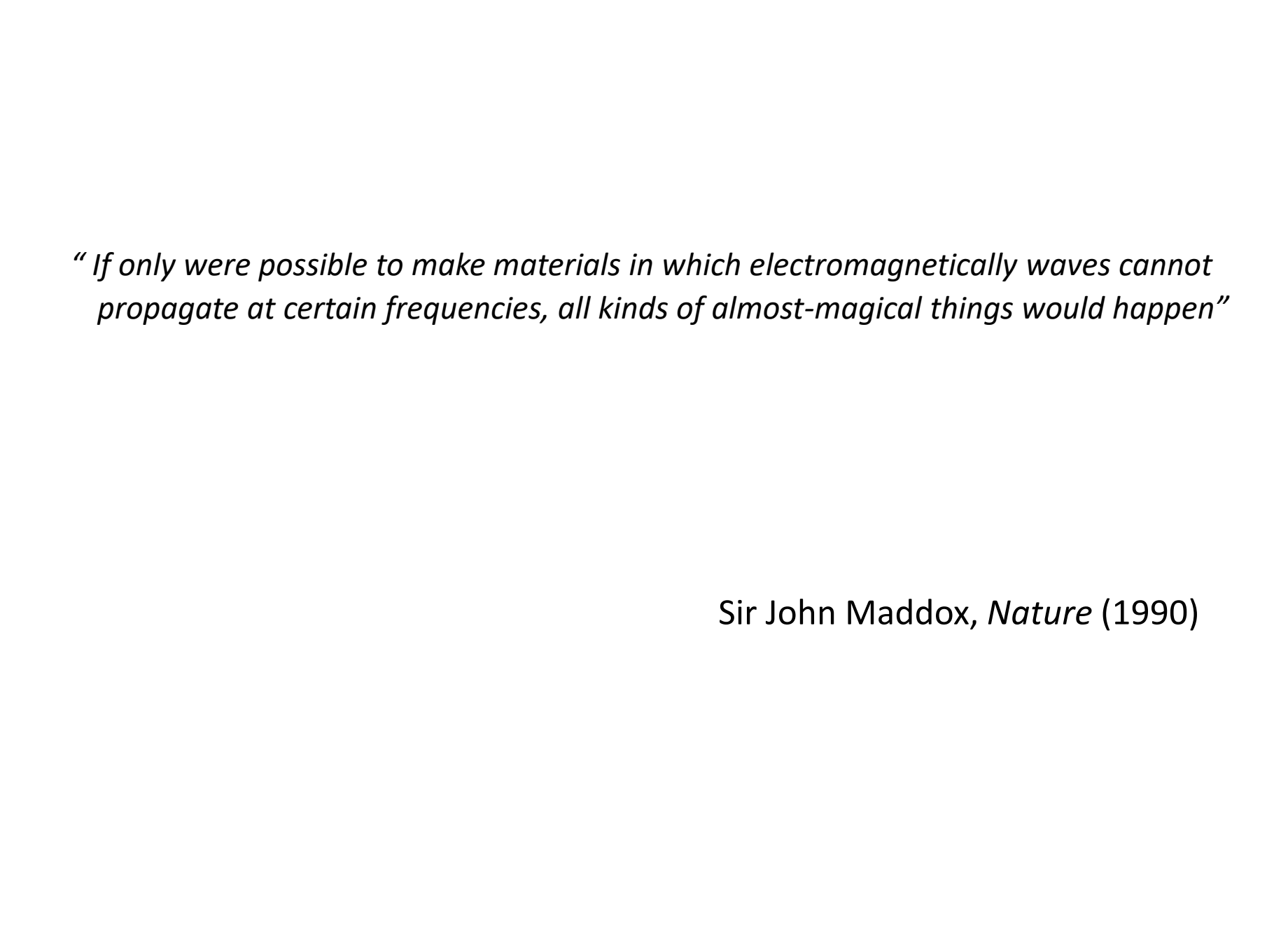


Length scale $\sim \lambda$

Artificial structures

Control EM wave propagation

New frontier in modern optics



Photonic Crystals History

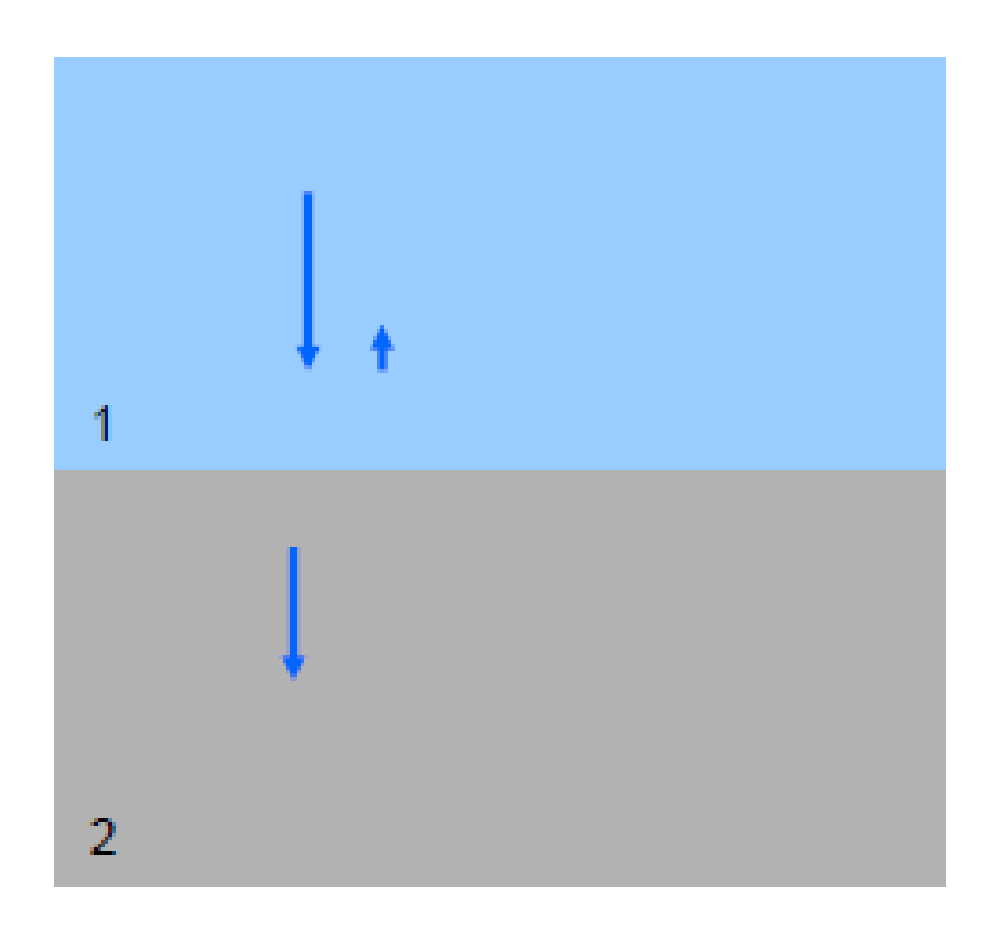
- 1987: Prediction of photonic crystals
 - S. John, Phys. Rev. Lett. **58**,2486 (1987), "Strong localization of photons in certain dielectric superlattices"
 - E. Yablonovitch, Phys. Rev. Lett. **58** 2059 (1987), "Inhibited spontaneous emission in solid state physics and electronics"
- 1990: Computational demonstration of photonic crystal

 K. M. Ho, C. T Chan, and C. M. Soukoulis, Phys. Rev. Lett. 65, 3152 (1990)
- 1991: Experimental demonstration of **microwave** photonic crystals E. Yablonovitch, T. J. Mitter, K. M. Leung, Phys. Rev. Lett. 67, 2295 (1991)
- 1995: "Large" scale 2D photonic crystals in **Visible**U. Gruning, V. Lehman, C.M. Englehardt, Appl. Phys. Lett. 66 (1995)
- 1998: "Small" scale photonic crystals in near Visible; "Large" scale inverted opals
- 1999: First photonic crystal based optical devices (lasers, waveguides)

Single interface reflection



light incident on layers with index mismatch ⇒ reflected wave (few percent)



$$r = \frac{n_1 + i\kappa_1 - n_2 - i\kappa_2}{n_1 + i\kappa_1 + n_2 + i\kappa_2}$$
$$= \frac{n_1 - n_2 + i(\kappa_1 - \kappa_2)}{n_1 + n_2 + i(\kappa_1 + \kappa_2)}$$

Note: exchange of 1 and 2 results in same denominator but opposite numerator $\Rightarrow \pi$ phase difference

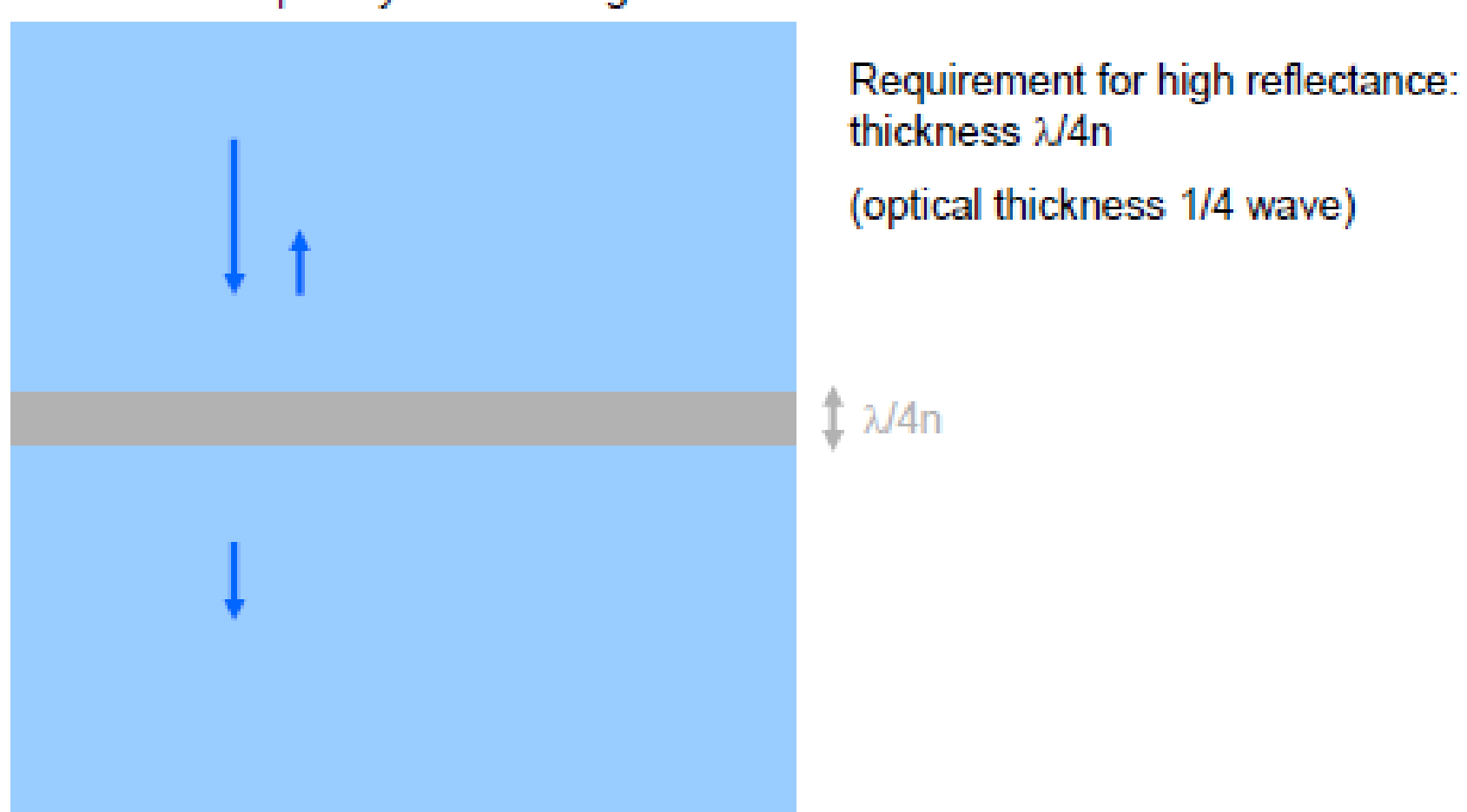
If n_1 =1, n_2 = 2, numerator ~ -1 sparse to dense $\Rightarrow \pi$ phase change

If $n_1=2$, $n_2=1$, numerator ~ 1 (real) dense to sparse $\Rightarrow \sim 0$ phase change

Double interface reflection

Light incident on two interfaces (thin layer with index higher than surroundings)

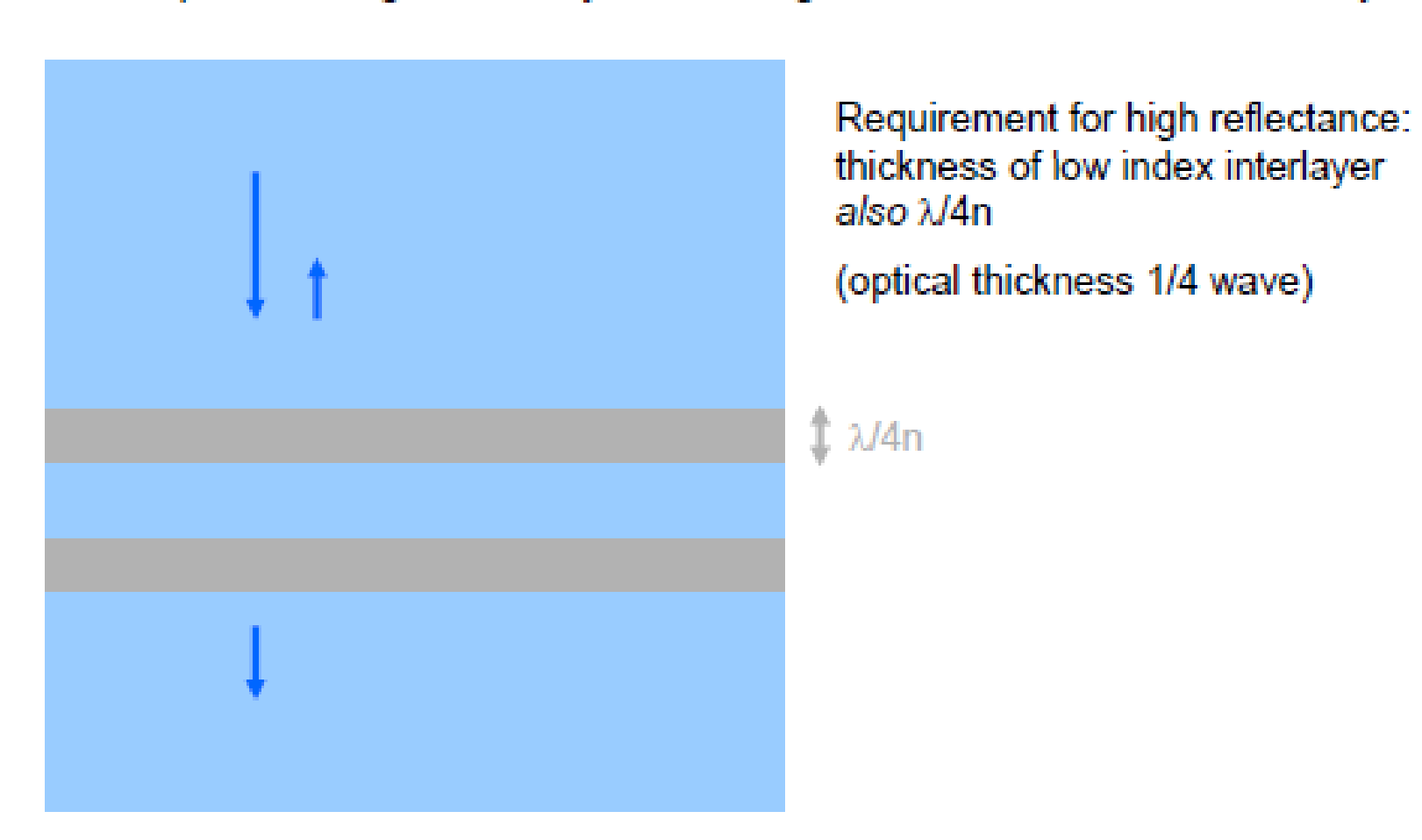
Reflection at first interface: π phase change second interface: 0 phase change \Rightarrow If total total $\Delta \varphi$ in layer is 180deg we obtain constructive reflective interference



Double interface reflection

Reflection from 2^{nd} interface: zero phase change; 3^{rd} interface: π phase change

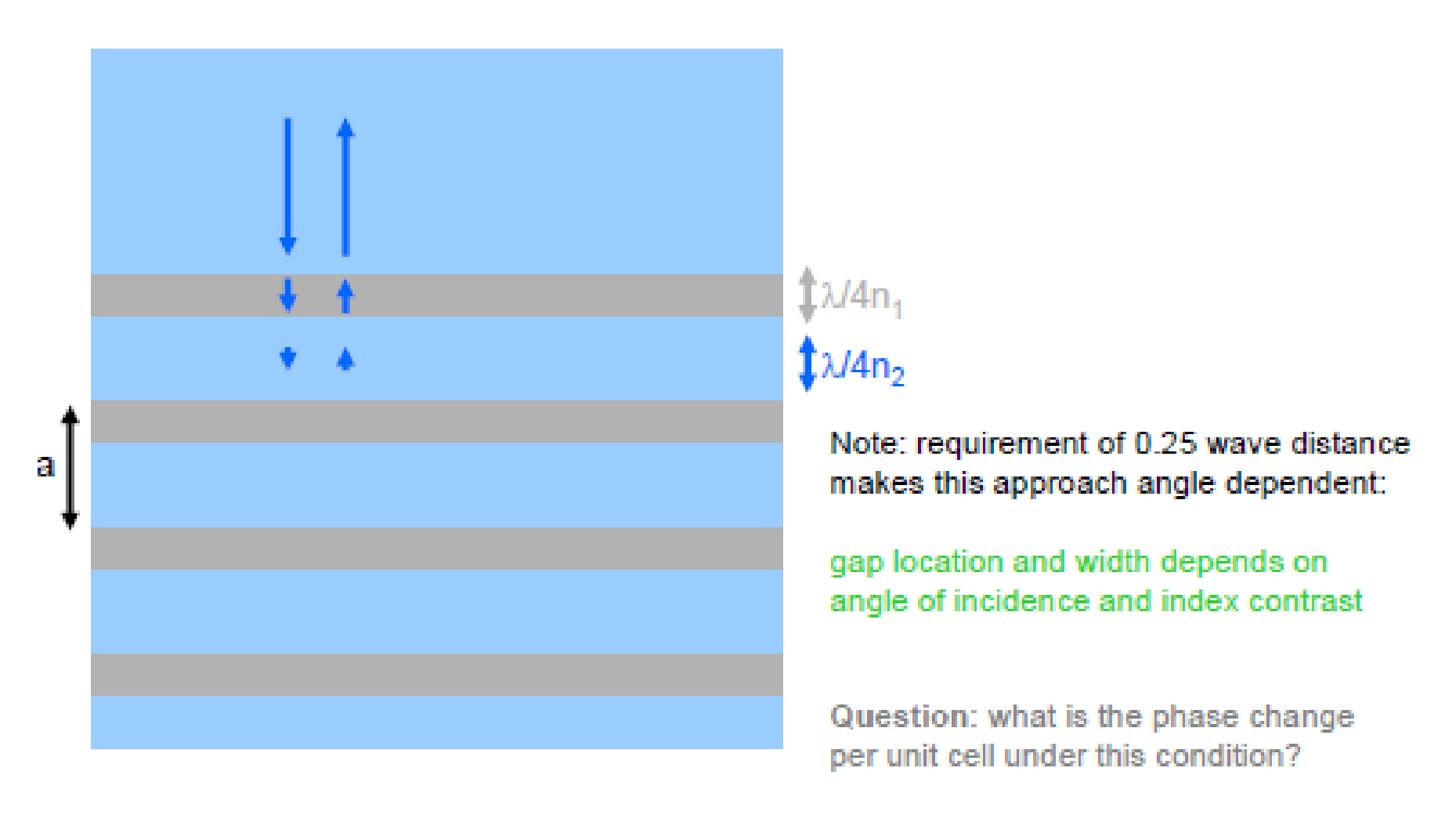
⇒ If total phase change in interlayer is 180deg : 2 and 3 interfere constructively



Reflection from many interfaces



light incident on series of interfaces all spaced λ/2n apart
⇒ reflected wave ~100%; no propagation in stack possible ⇒ 1D bandgap



Contrast dependent band gap

C

Magnitude of the bandgap depends on index contrast

No contrast, no reflections, no gap

Weak contrast, reflected beam only enhanced if many interfaces contribute with exactly the correct phase: highly frequency selective: small gap

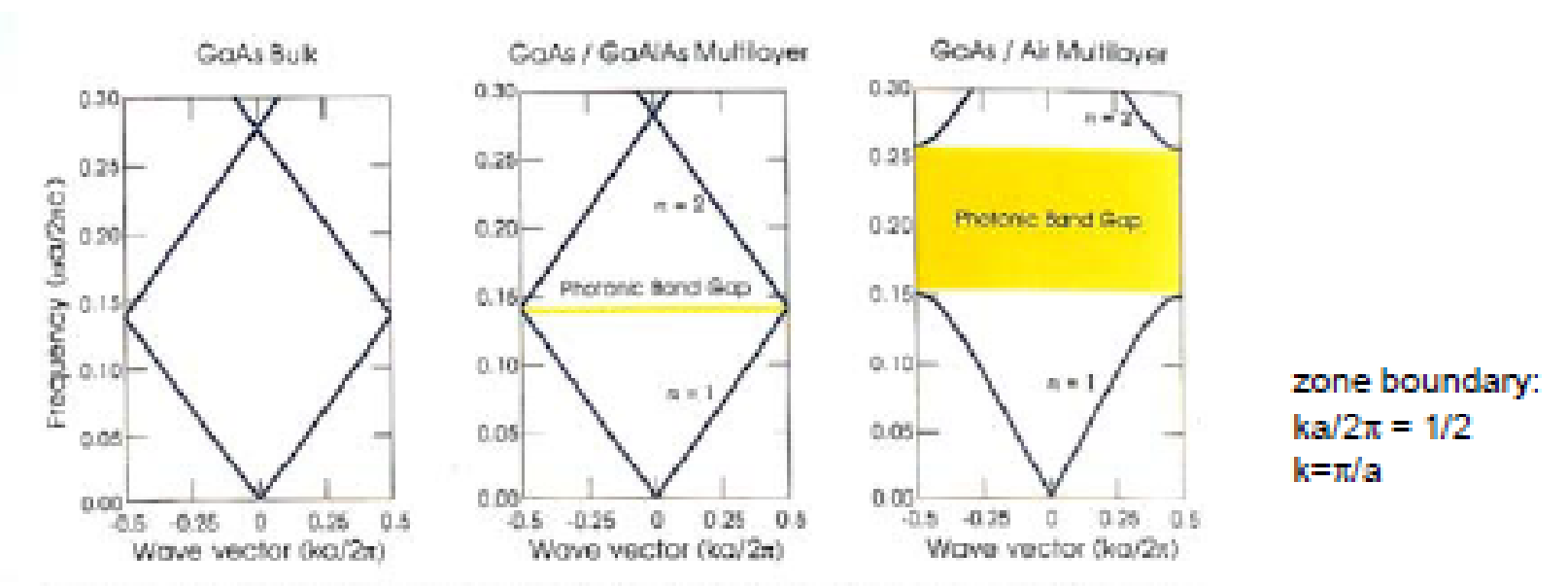


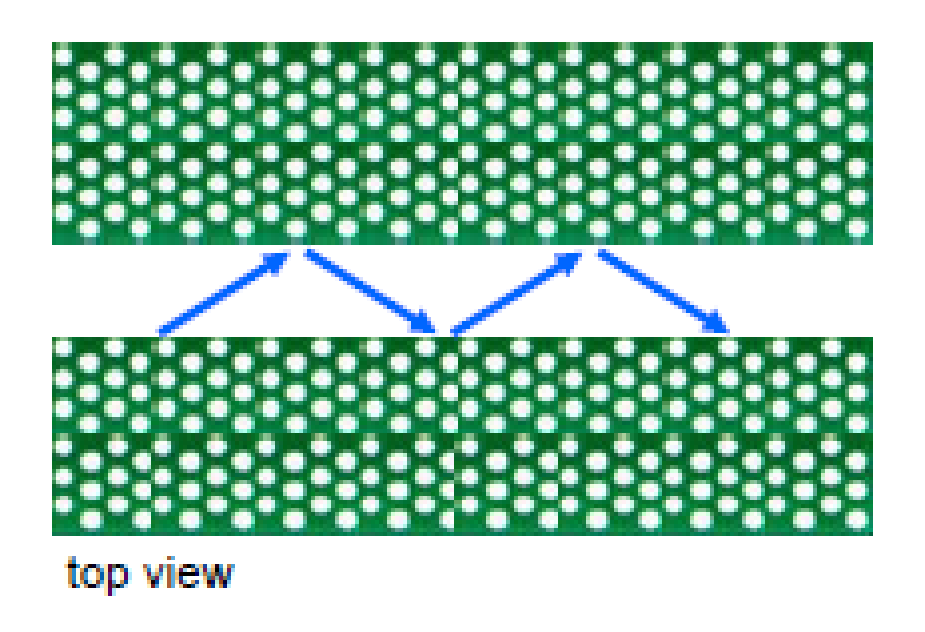
Figure 2 The photonic band structures for on-axis propagation, shown for three different multilayer films, all at which have layers of width 0.5a. Left: each layer has the same dielectric constant $\varepsilon=13$. Center: layers afternate between $\varepsilon=13$ and $\varepsilon=12$. Right: layers afternate between $\varepsilon=13$ and $\varepsilon=1$.

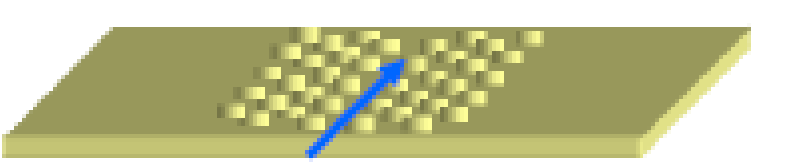
From: Photonic Crystals – Molding the flow of light, Joannopoulos, Meade, and Winn

Mode confinement

Light propagation at center of bandgap: 'external reflection' due to destructive interference inside periodic lattice ⇒ guiding in 'line defect' possible

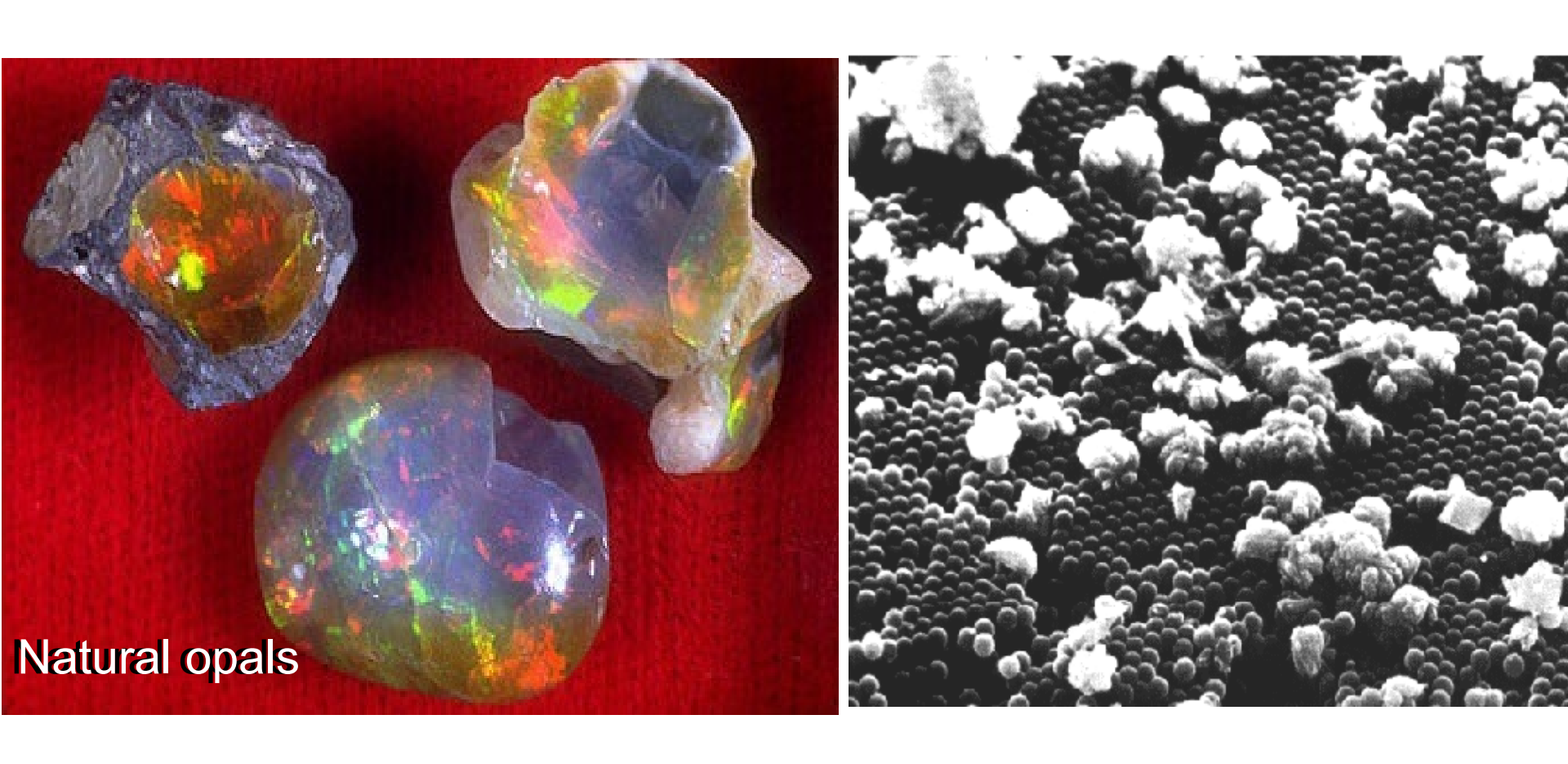
Note: vertical confinement achieved here by conventional index guiding





Patterned membrane

Natural Photonic Crystals: Structural Colors through Photonic Crystals



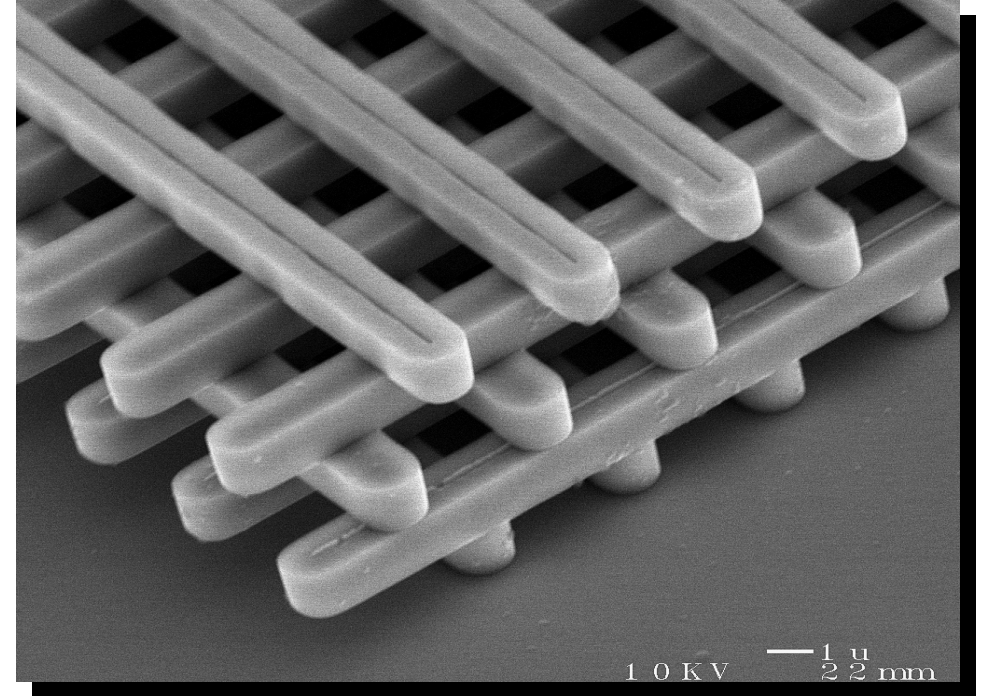
Periodic structure → striking color effect even in the absence of pigments

Artificial Photonic Crystals

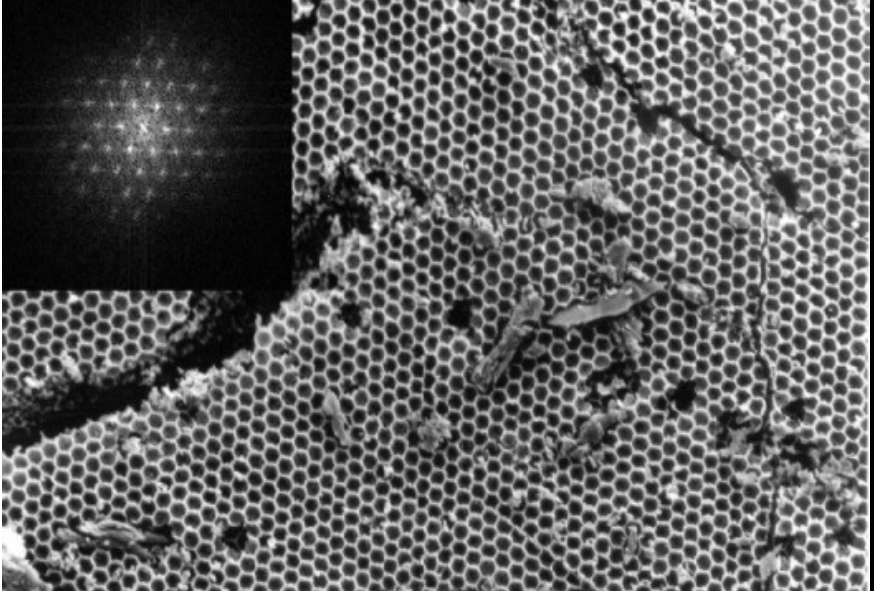
Requirement: overlapping of frequency gaps along different directions

- High ratio of dielectric indices
- Same average optical path in different media
- Dielectric networks should be connected

Woodpile structure



S. Lin et al., Nature (1998)

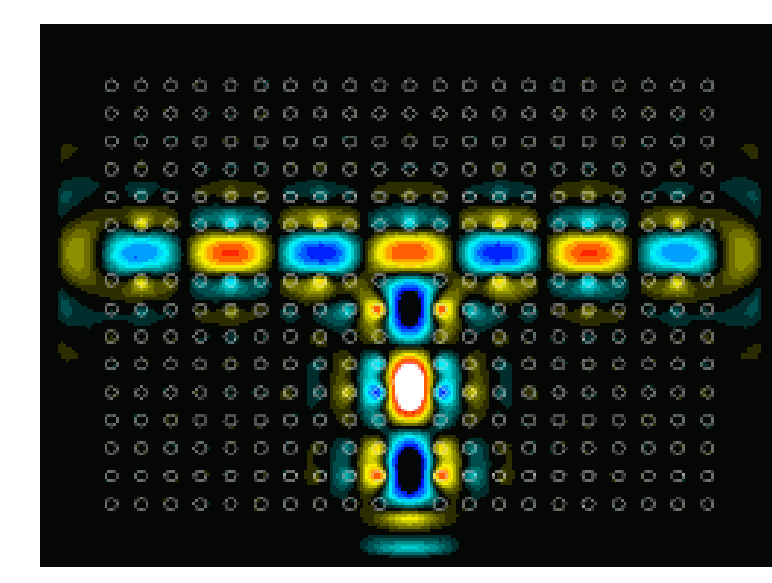


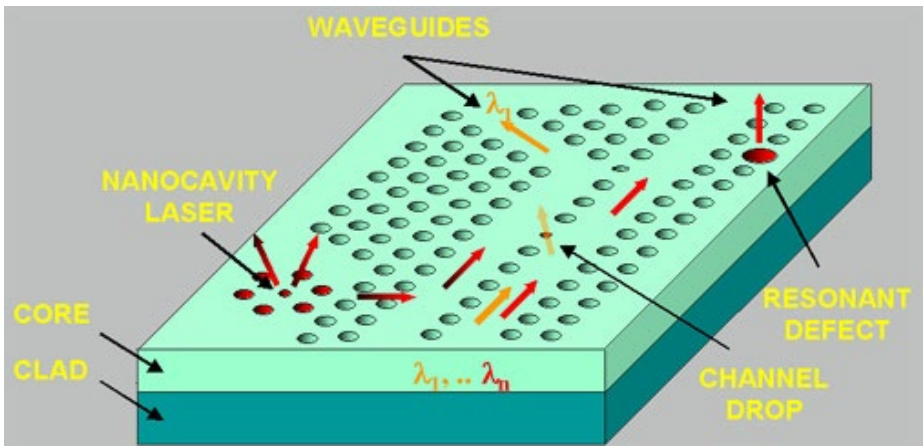
Inverted Opals

J. Wijnhoven & W. Vos, Science (1998)

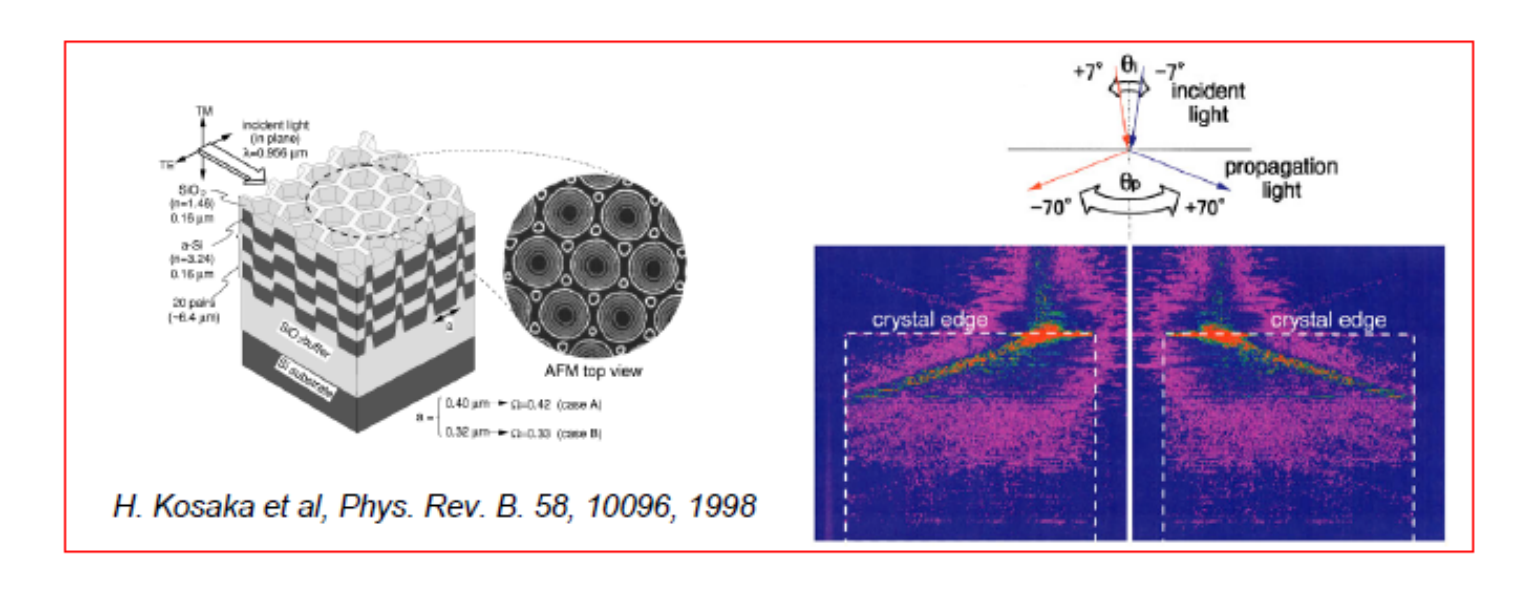
Photonic Crystals: Opportunities

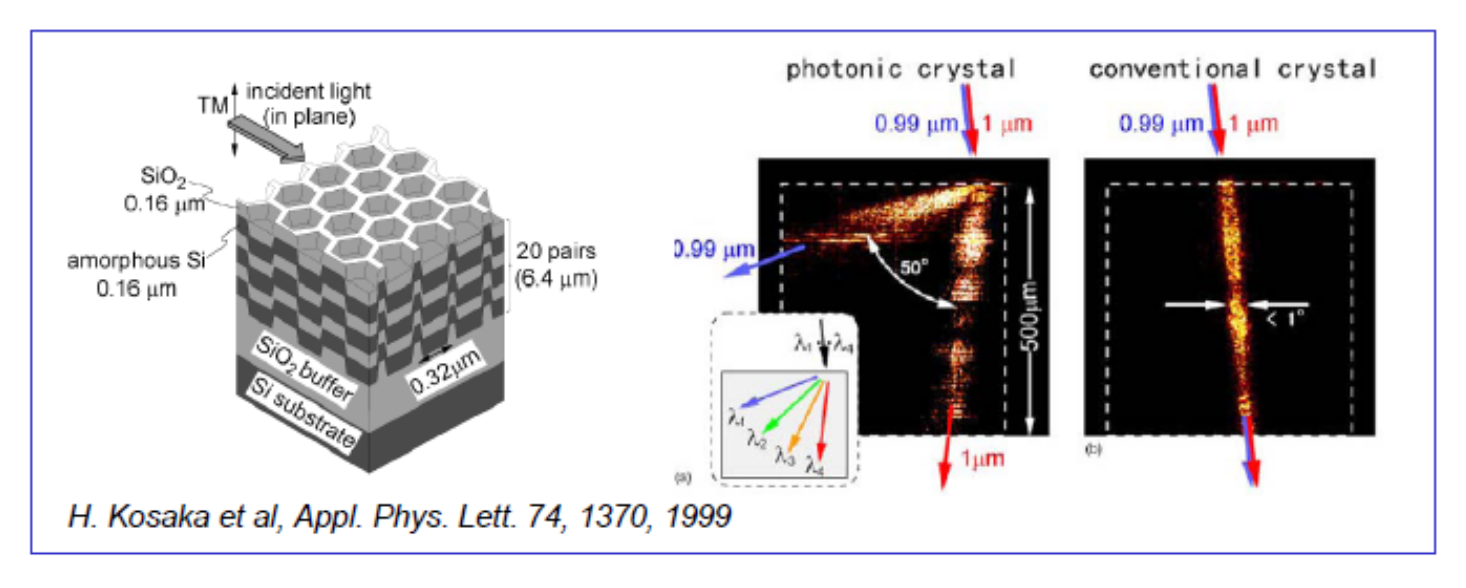
- Photonic Crystals
 - complex dielectric environment that controls the flow of radiation
 - designer vacuum for the emission and absorption of radiation
- Passive devices
 - dielectric mirrors for antennas
 - micro-resonators and waveguides
- Active devices
 - low-threshold nonlinear devices
 - microlasers and amplifiers
 - efficient thermal sources of light
- Integrated optics
 - controlled miniaturisation
 - pulse sculpturing





Super-lens and Super-prism effects

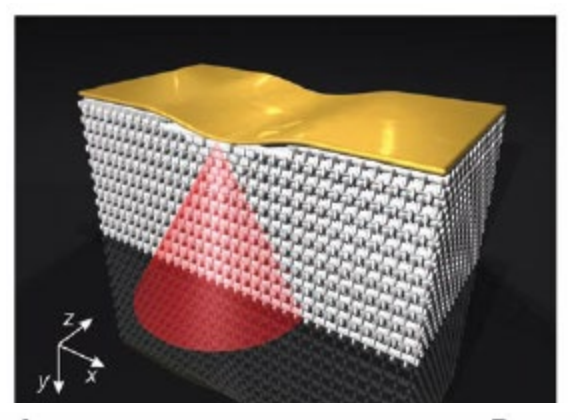


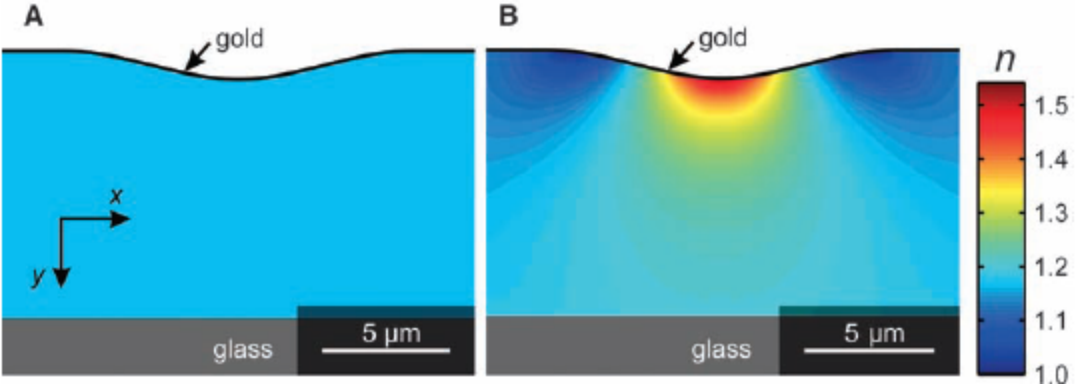


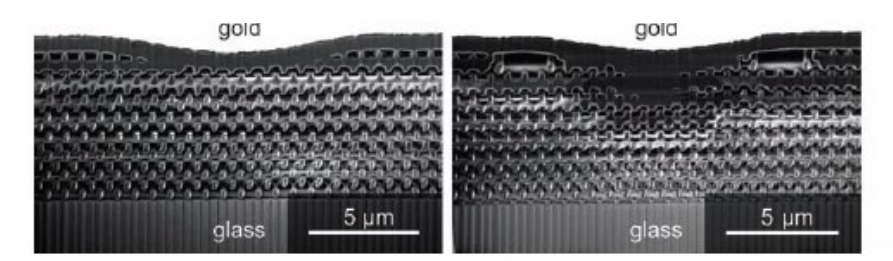
Three-Dimensional Invisibility Cloak at Optical Wavelengths

Tolga Ergin, 1,2* † Nicolas Stenger, 1,2* Patrice Brenner, 2 John B. Pendry, 3 Martin Wegener 1,2,4

We have designed and realized a three-dimensional invisibility-cloaking structure operating at optical wavelengths based on transformation optics. Our blueprint uses a woodpile photonic crystal with a tailored polymer filling fraction to hide a bump in a gold reflector. We fabricated structures and controls by direct laser writing and characterized them by simultaneous high—numerical-aperture, far-field optical microscopy and spectroscopy. A cloaking operation with a large bandwidth of unpolarized light from 1.4 to 2.7 micrometers in wavelength is demonstrated for viewing angles up to 60°.







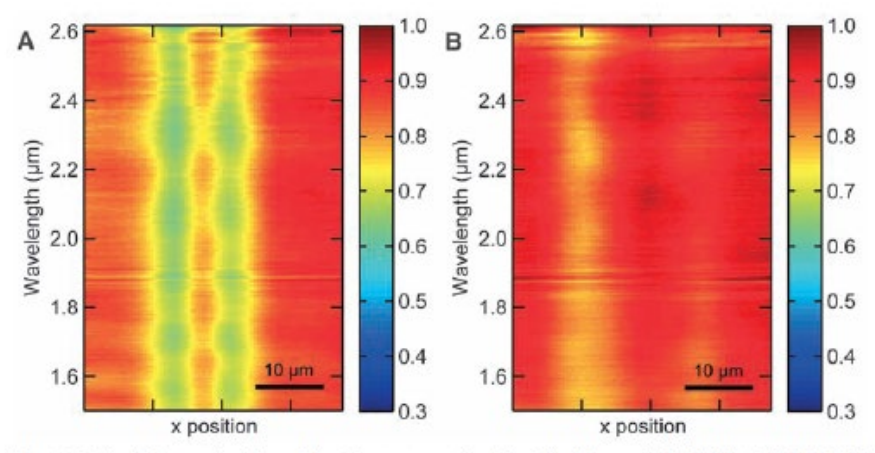


Fig. 3. Optical characterization of the 3D structures (see Fig. 2) with unpolarized light in bright-field mode. The image intensity is shown on a false-color scale. The horizontal axis is a cut through the middle of the structure along the *x* direction (compare to Fig. 1A); the vertical axis is wavelength. (**A**) A bump without a cloak. The bump is immediately visible. (**B**) Result for a bump with a doak that approaches the expectation for an ideal cloak (constant intensity).

Fig. 2. Target refractive index (n) distributions (top) and oblique-view electron micrographs of fabricated structures after FIB milling (bottom). (A) A bump without a cloak. (B) A bump with a cloak. Note that the oblique view in the electron micrographs compresses the y direction.

Science 328, 327 (2010)

insight review articles

Photonic structures in biology

Pete Vukusic and J. Roy Sambles

Thin Film Photonics, School of Physics, Exeter University, Exeter EX44QL, UK (e-mail: P.Vukusic@ex.ac.uk)

Millions of years before we began to manipulate the flow of light using synthetic structures, biological systems were using nanometre-scale architectures to produce striking optical effects. An astonishing variety of natural photonic structures exists: a species of Brittlestar uses photonic elements composed of calcite to collect light, *Morpho* butterflies use multiple layers of cuticle and air to produce their striking blue colour and some insects use arrays of elements, known as nipple arrays, to reduce reflectivity in their compound eyes. Natural photonic structures are providing inspiration for technological applications.

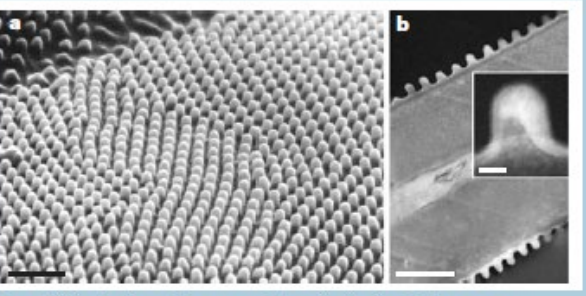


Figure 7 Anti-reflective nipple arrays. a, The anti-reflective nipple arrays on ommatidial surfaces of a lepidopteran eye appear identical to those found (b) on the transparent wings of certain hawkmoths. This image shows a transparent wing section with a nipple array on both surfaces. The inset image shows the magnified profile of a single nipple. Bars. a, 1 mm; b, 1 mm; inset, 100 nm.

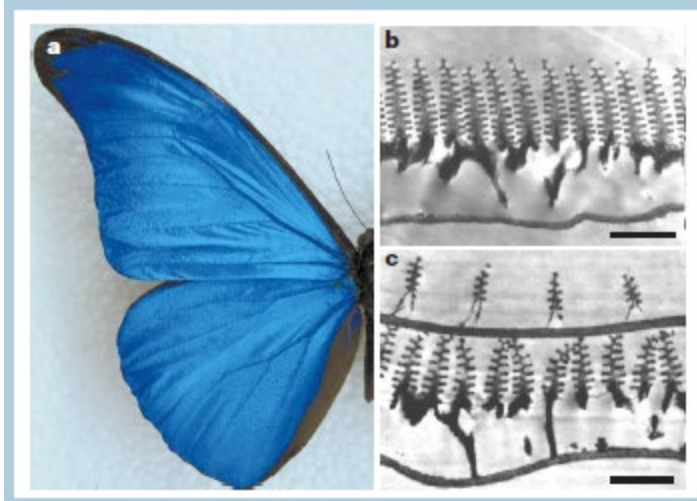


Figure 3 Iridescence in the butterfly *Morpho rhetenor*. **a**, Real colour image of the blue iridescence from a *M. rhetenor* wing. **b**, Transmission electron micrograph (TEM) images showing wing-scale cross-sections of *M. rhetenor*. **c**, TEM images of a wing-scale cross-section of the related species *M. dīdīus* reveal its discretely configured multilayers. The high occupancy and high layer number of *M. rhetenor* in **b** creates an intense reflectivity that contrasts with the more diffusely coloured appearance of *M. dīdīus*, in which an overlying second layer of scales effects strong diffraction⁴. Bars, **a**, 1 cm; **b**, 1.8 μm; **c**, 1.3 μm.

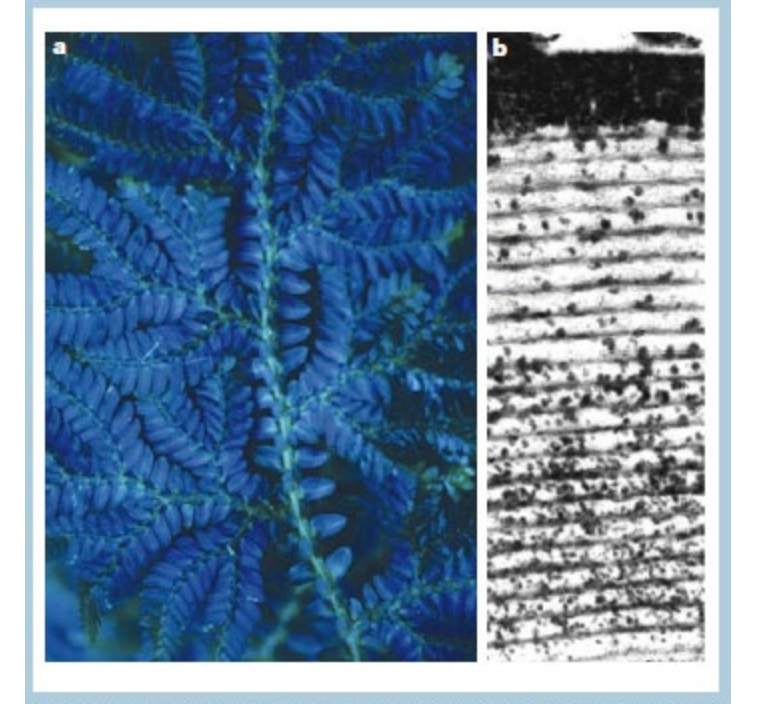


Figure 5 Structural colour in flora. **a**, Blue irridescence is prevalent in the fern-like tropical understory plants of the genus *Selaginella*. **b**, TEM section of a juvenile leaf from the plant *Diplazium tomentosum*. (Both images reproduced with permission from D. Lee.)

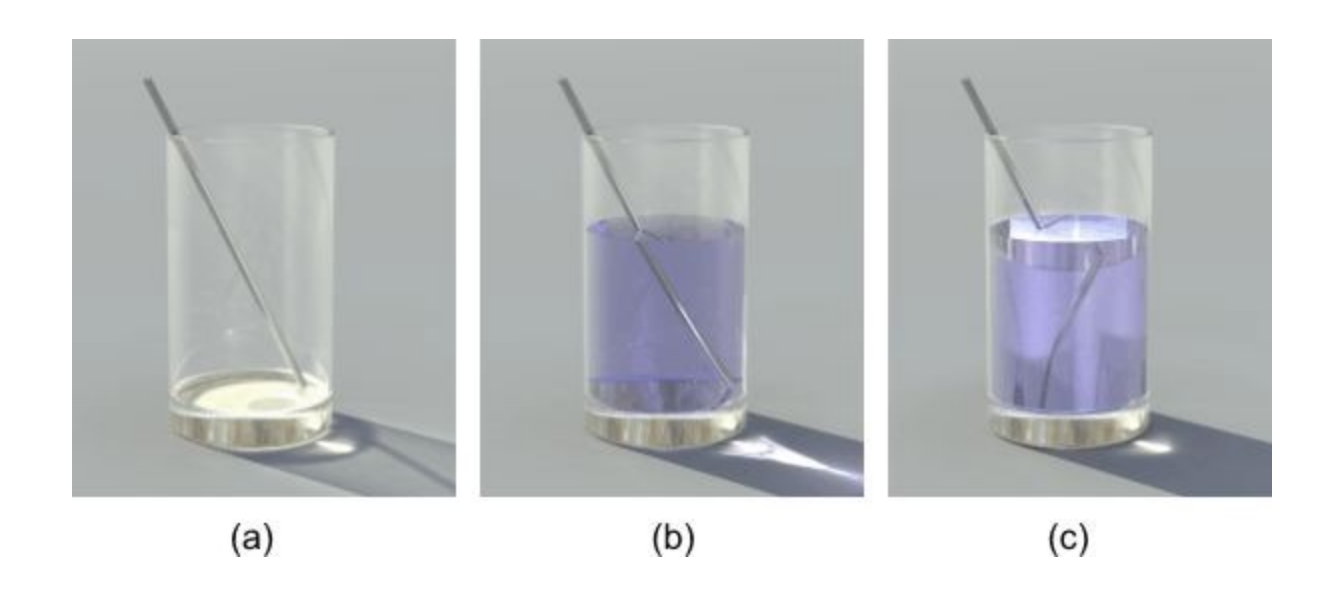
Purdue university—Nanophotonics & Metamaterials ECE 695s

http://cobweb.enc.purdue.edu/~ece695s

D.R. Smith at Duke University—

http://people.ee.duke.edu/~drsmi th/pubs_smith.htm

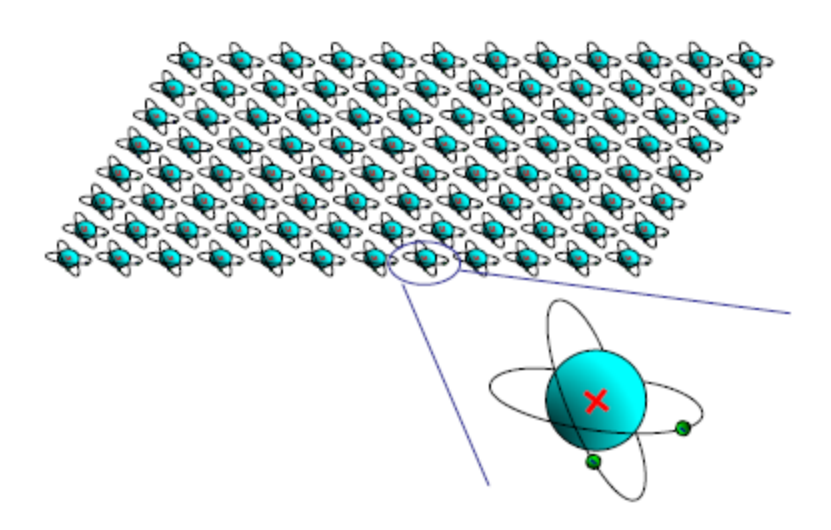
Metamaterials. Negative refraction.



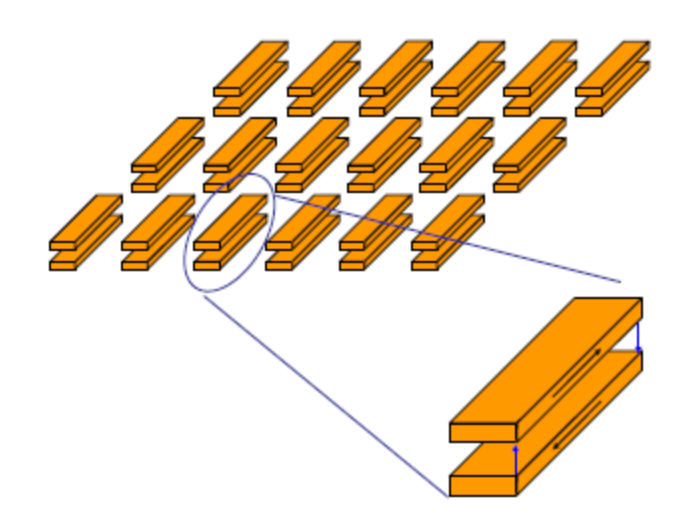
What is a metamaterial?

Metamaterials are engineered composites tailored for specific electromagnetic properties that are not found in nature and not observed in the constituent materials

μετα = meta = beyond (Greek)

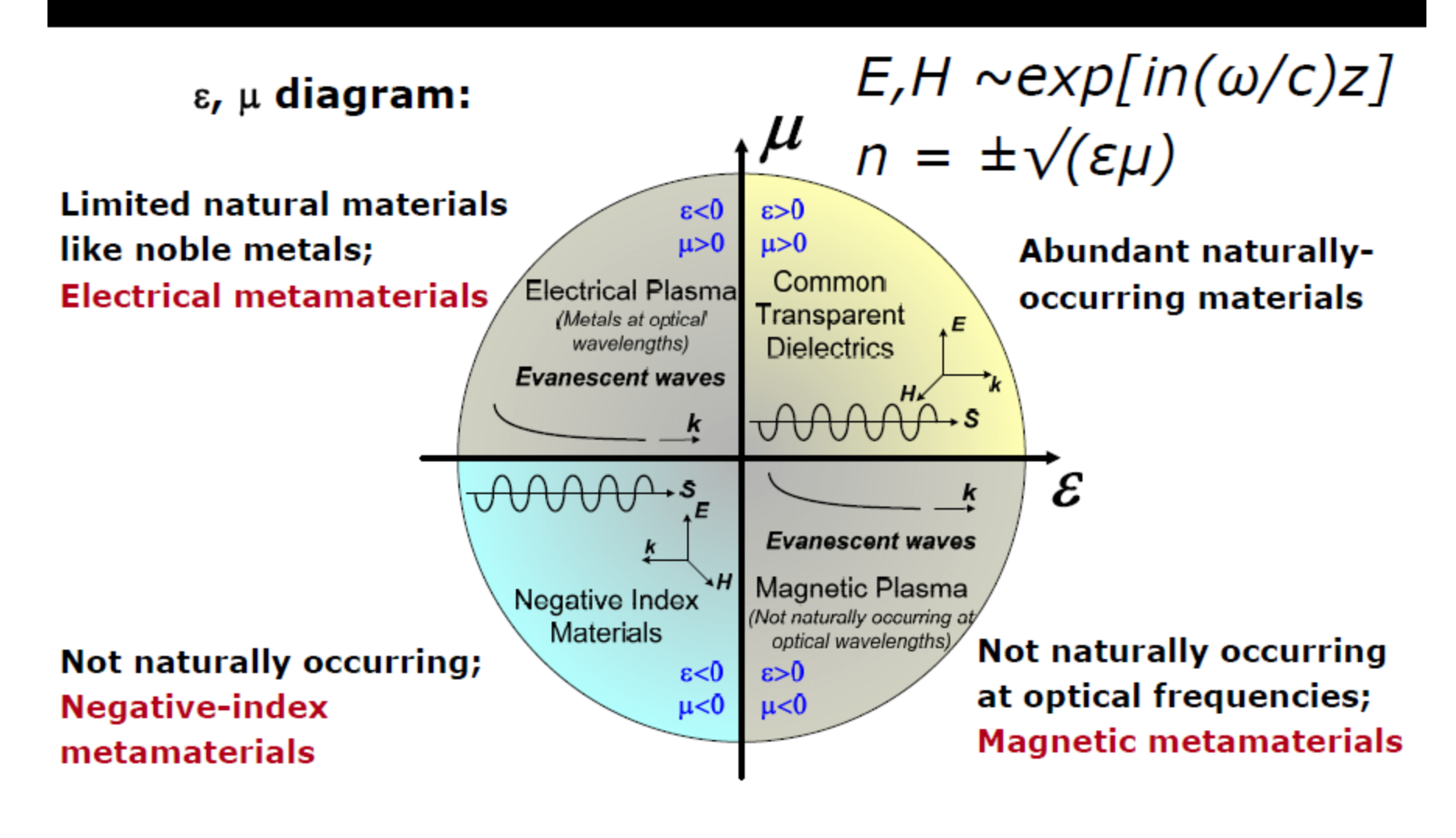


A natural material with its atoms



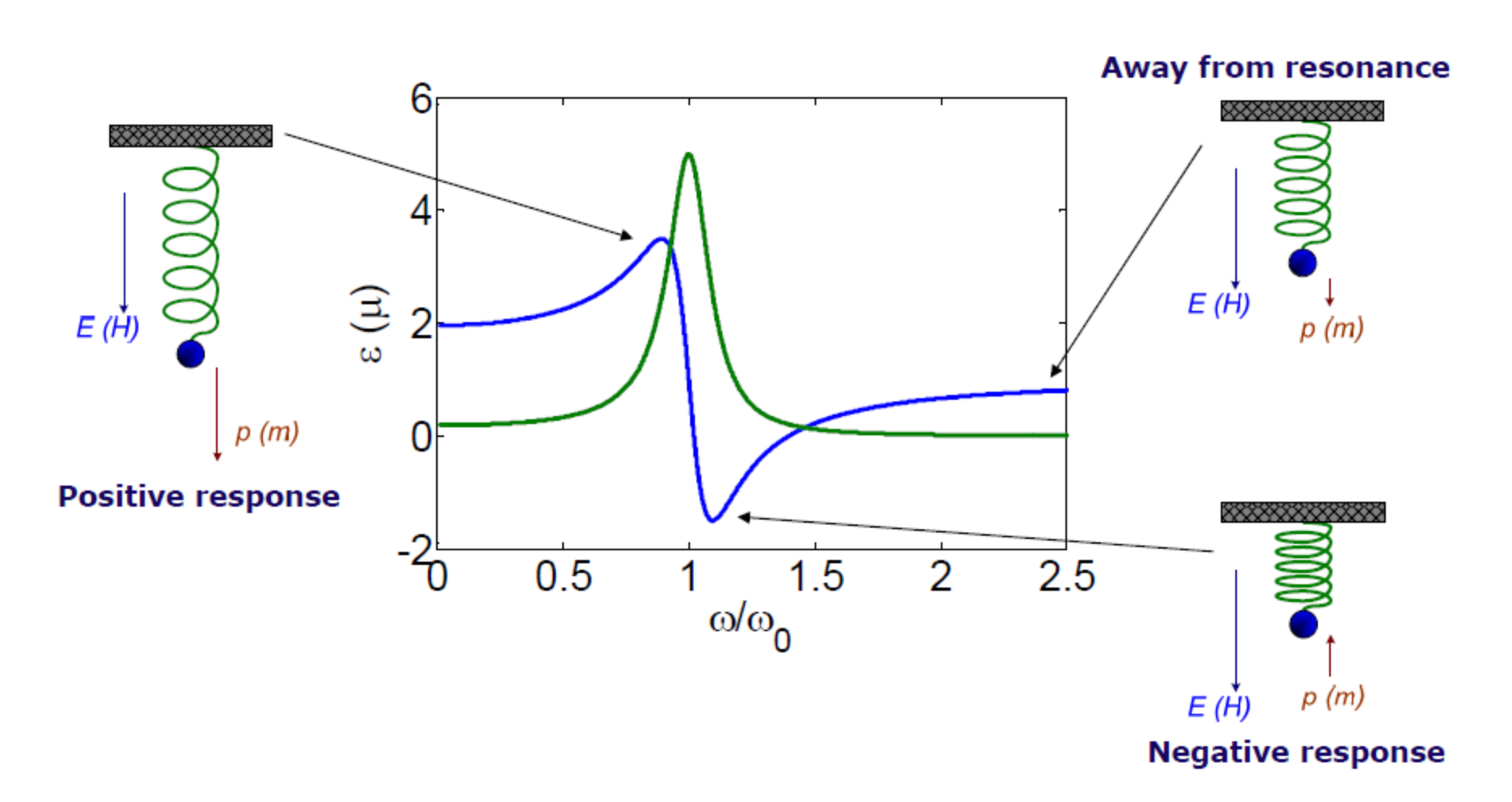
A metamaterial with artificially structured "atoms"

Why need metamaterials?



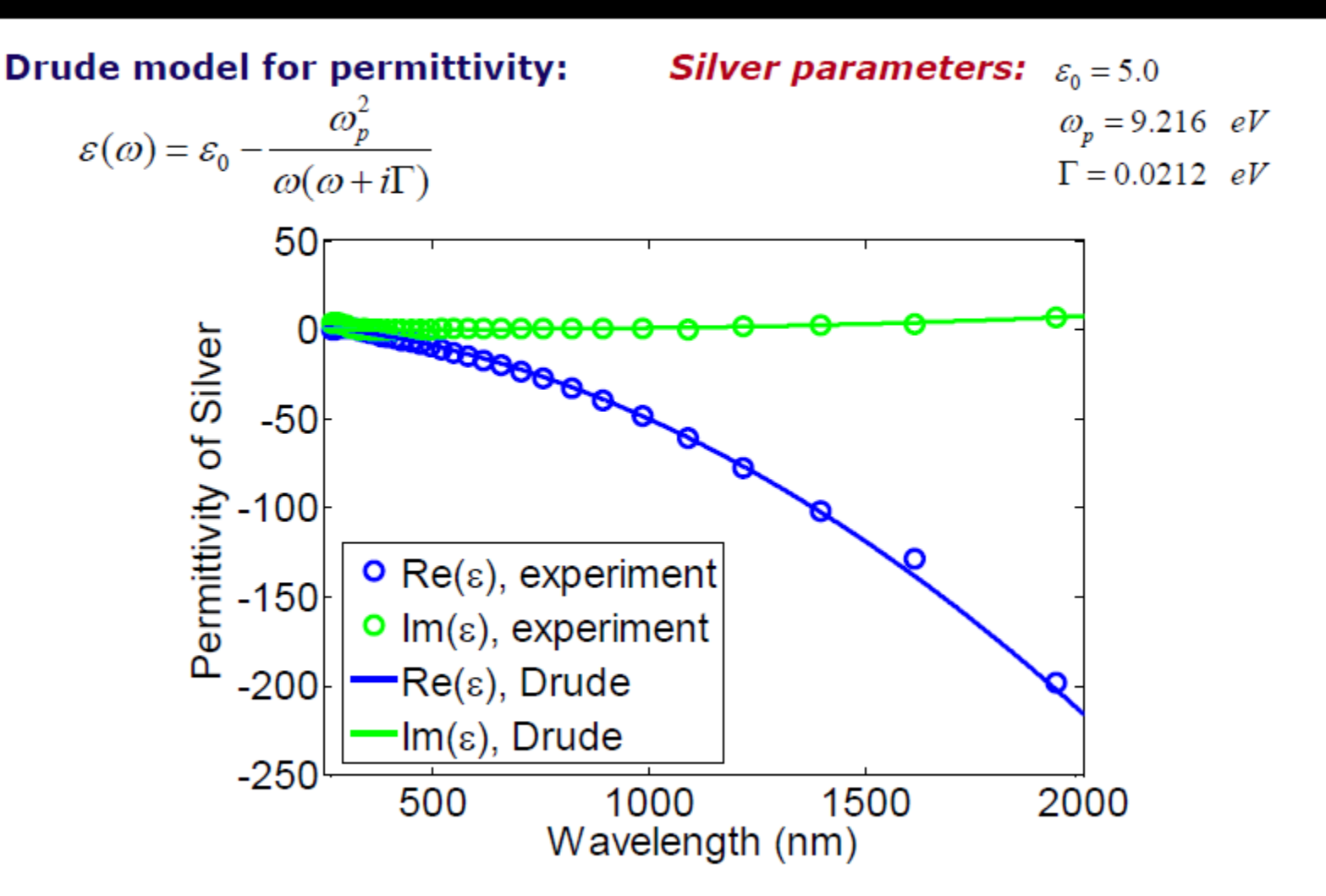
General properties of electromagnetic resonances

Resonance described by Lorentz line shape



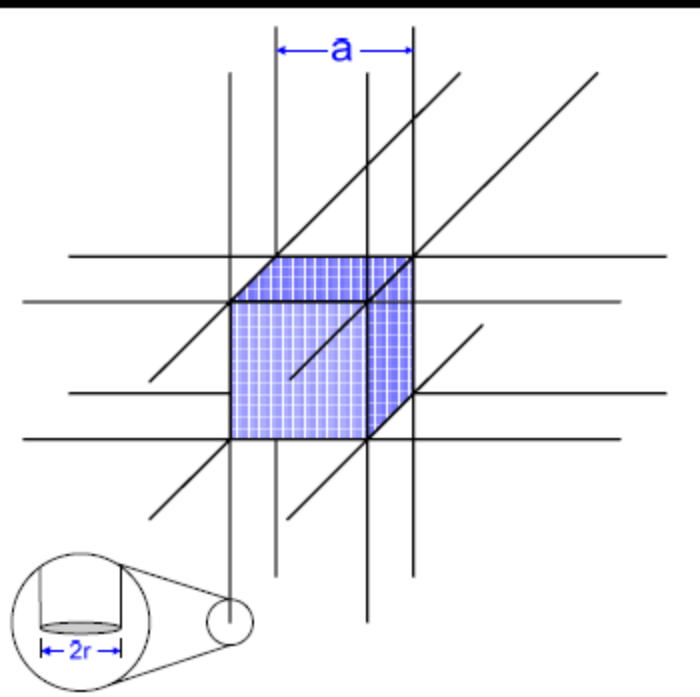
Electrical metamaterials

Drude model for noble metal: negative ε in nature



Experimental data from Johnson & Christy, PRB, 1972

Example of electrical metamaterials: metal wires arrays



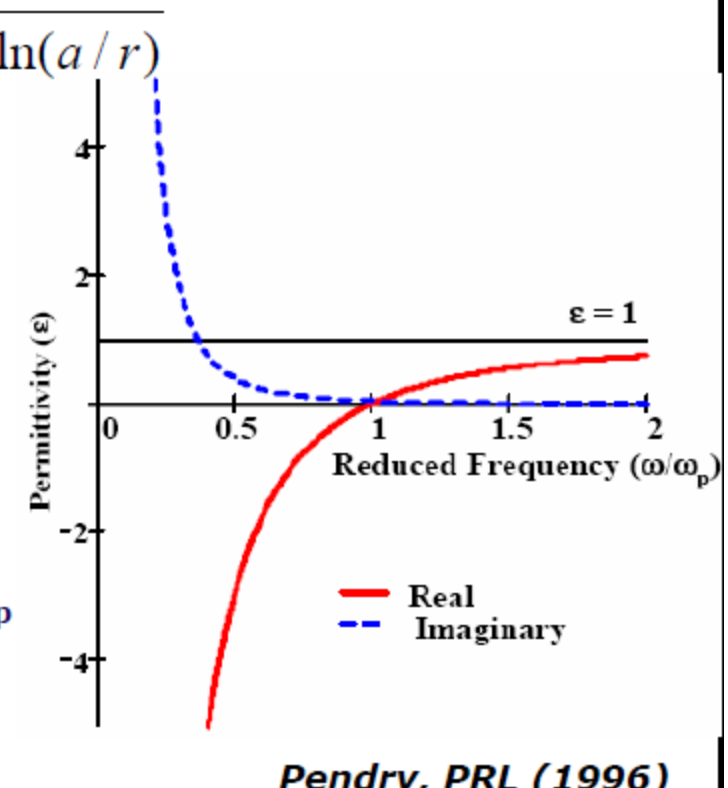
$$\varepsilon = \varepsilon' + i\varepsilon'' = 1 - \frac{\omega_p^2}{\omega(\omega + i\varepsilon_0 a^2 \omega_p^2 / \pi r^2 \sigma)}$$

$$\omega_p^2 = \frac{2\pi c^2}{a^2 \ln(a/r)}$$

A periodic array of thin metal wires with $r < a < < \lambda$ acts as a low frequency plasma

The effective ε is described with modified ω_p

Plasma frequency depends on geometry rather than on material properties



Pendry, PRL (1996)

Magnetic metamaterials

Optical magnetic response: a missing hand of light in nature

```
Natural magnetic responses (Ferromagnetic / Ferrimagnetic / Antiferromagnetic resonances) typically occur at lower than a few GHz
```

There are no free magnetic monopoles; therefore no magnetic plasma

All conventional optics (lenses, mirrors, crystals, ...) essentially have nothing to do with magnetic fields

```
Magnetic coupling to an atom: \sim \mu_B = e\hbar/2m_e c = \alpha e a_0 (Bohr magneton)

Electric coupling to an atom: \sim e a_0

Magnetic effect / electric effect \approx \alpha^2 \approx (1/137)^2
```

"... the magnetic permeability $\mu(\omega)$ ceases to have any physical meaning at relatively low frequencies...there is certainly no meaning in using the magnetic susceptibility from optical frequencies onwards, and in discussion of such phenomena we must put μ =1."

Landau and Lifshitz, ECM, Chapter 79.

Negative permeability

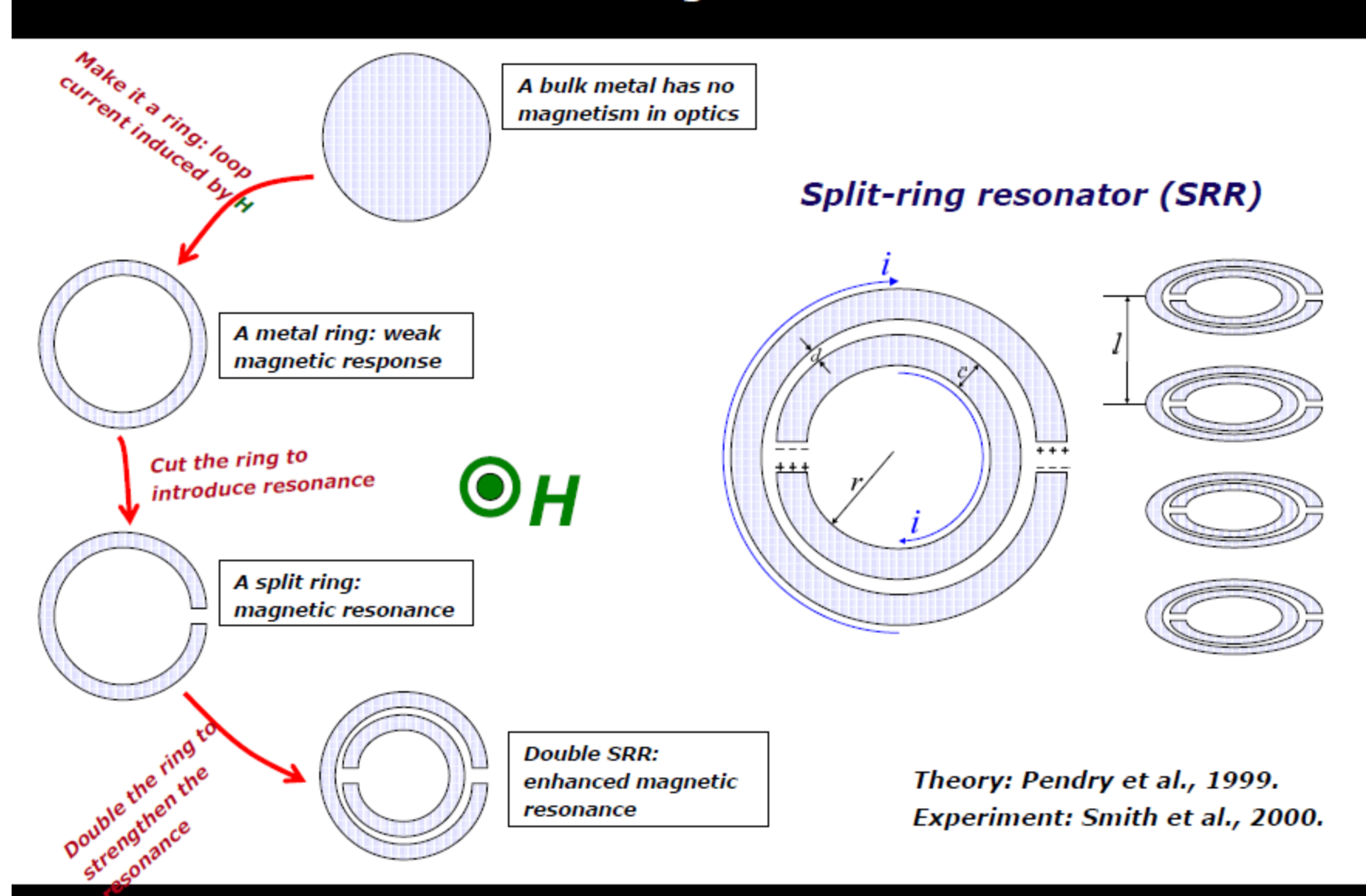
Negative ε can be obtained in metals (recall Drude model, Lorentz model) but negative (isotropic) μ does not appear to occur in nature

Magnetism from Conductors and Enhanced Nonlinear Phenomena,
J. B. Pendry et. al, IEEE Transaction on microwave theory and techniques 47, 2075 (1999)

Abstract—We show that microstructures built from nonmagnetic conducting sheets exhibit an effective magnetic permeability μ_{-μ}, which can be tuned to values not accessible in naturally occurring materials, including large imaginary components of $\mu_{\rm eff}$. The microstructure is on a scale much less than the wavelength of radiation, is not resolved by incident microwaves, and uses a very low density of metal so that structures can be extremely lightweight. Most of the structures are resonant due to internal capacitance and inductance, and resonant enhancement combined with compression of electrical energy into a very small volume greatly enhances the energy density at critical locations in the structure, easily by factors of a million and possibly by much more. Weakly nonlinear materials placed at these critical locations will show greatly enhanced effects raising the possibility of manufacturing active structures whose properties can be switched at will between many states.

Index Terms— Effective permeability, nonlinearity, photonic crystals.

SRR: the first magnetic metamaterials



Calculations of isotropic structure

Approach: dense array of split rings:

Planer splitting structure inner radius = 2.0mm width of each ring = 1.0mm spacing between ring edges = 0.1 mm lattice constant = 10.0mm

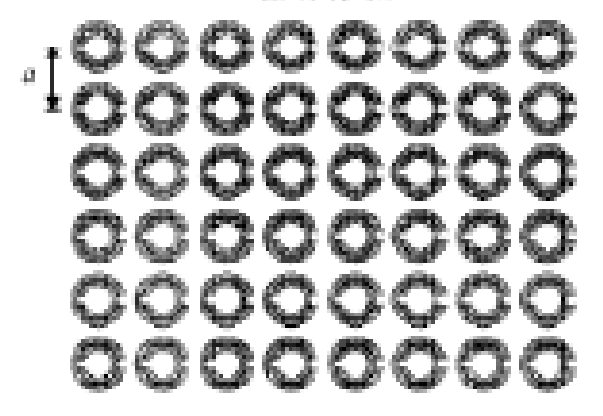


Fig. 13. Plain view of a split ring structure in a square array (lattice spacing a).

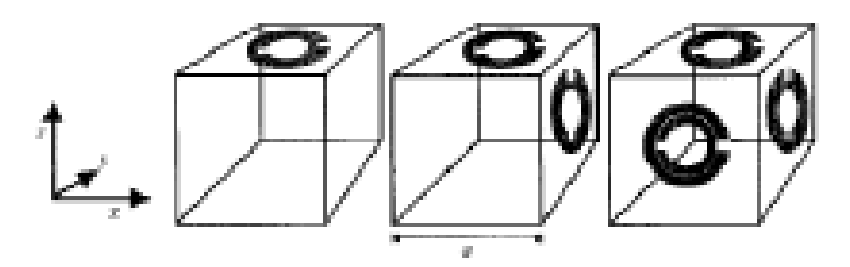
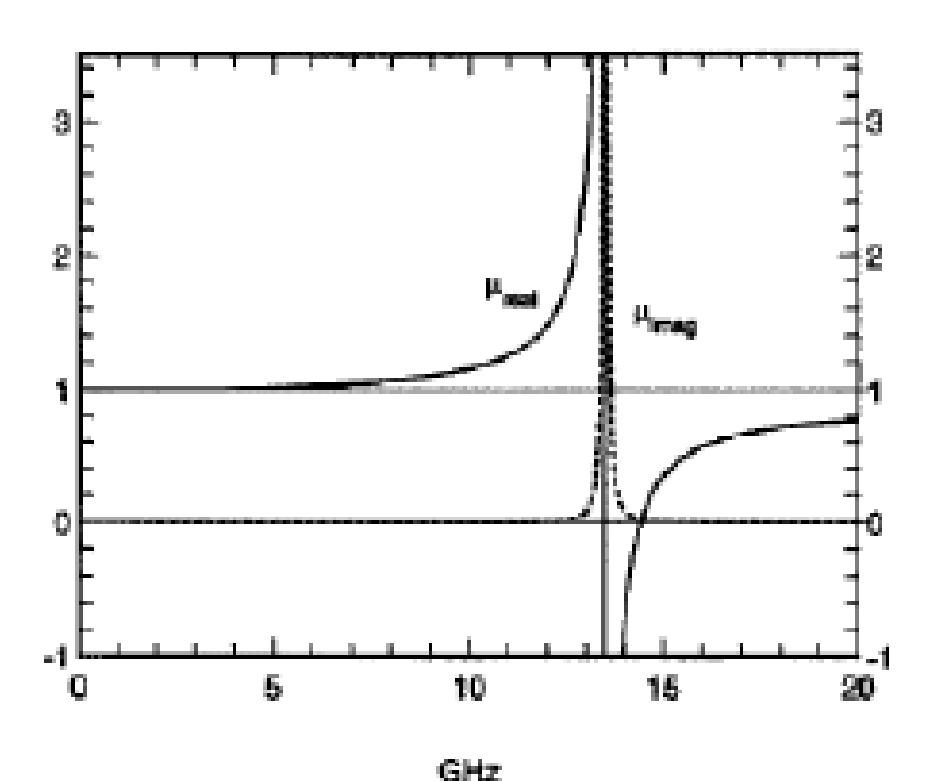


Fig. 14. Building 3-D symmetry: each successive restacking of the structure adds a mass to another side of the unit cell.

Calculated response for copper split rings shows resonance at GHz (10 GHz ⇒ λ ~ 3 cm > lattice spacing)



Negative-index metamaterials

Negative refractive index: A historical review





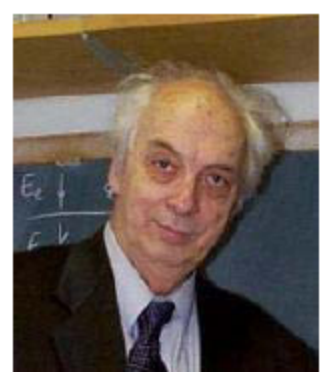
... energy can be carried forward at the group velocity but in a direction that is anti-parallel to the phase velocity... Schuster, 1904

Sir Arthur Schuster Sir Horace Lamb

Negative refraction and backward propagation of waves Mandel'stam, 1945



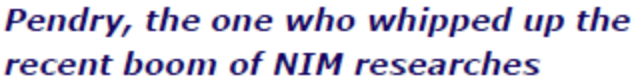
L. I. Mandel'stam



V. G. Veselago

Left-handed materials: the electrodynamics of substances with simultaneously negative values of ε and μ

Veselago, 1968



Low frequency plasmonic structure (1996) High frequency magnetic structure (1999) Perfect lens (2000) Optical cloaking (2006)



Sir John Pendry

Left-handed media (LHM): materials with negative ε and negative μ

Victor Veselago first discussed the properties of materials with negative ϵ and μ :

THE ELECTRODYNAMICS OF SUBSTANCES WITH SIMULTANEOUSLY NEGATIVE

VALUES OF & AND µ

V. G. VESELAGO

P. N. Lebedev Physics Institute, Academy of Sciences, U.S.S.B.

1. INTRODUCTION

THE dielectric constant ϵ and the magnetic permeability μ are the fundamental characteristic quantities which determine the propagation of electromagnetic waves in matter. This is due to the fact that they are the only parameters of the substance that appear in the dispersion equation

$$\left|\frac{ds^2}{ds^2}e_{ij}a_{i,j} - h^2b_{i,j} + h_ia_j\right| = 0,$$
 (2)

which gives the connection between the frequency ω of a monochromatic wave and its wave vector k. In the case of an isotropic substance, Eq. (1) takes a simpler form:

$$\frac{1}{2} = \frac{4d^2}{d^2} H^2$$
. (2)

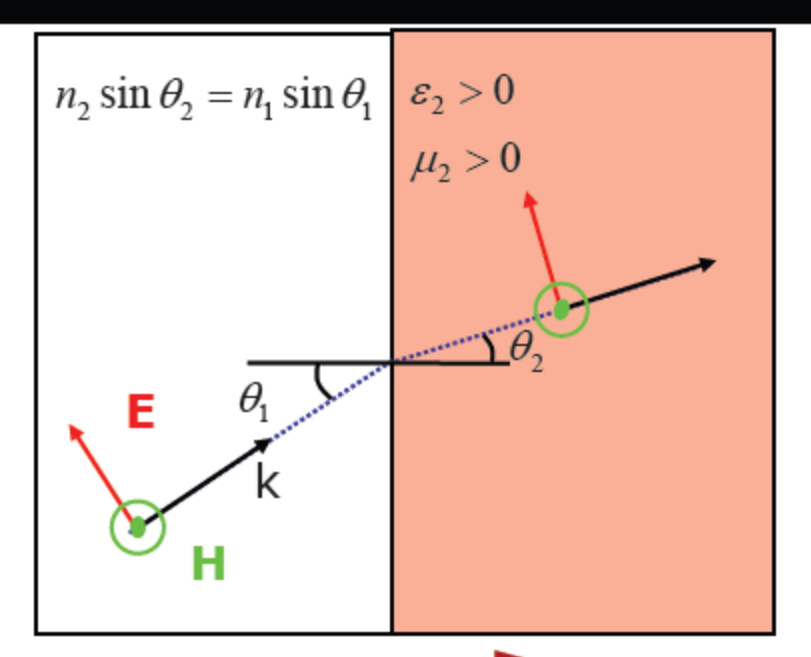
Here n² is the square of the index of refraction of the substance, and is given by

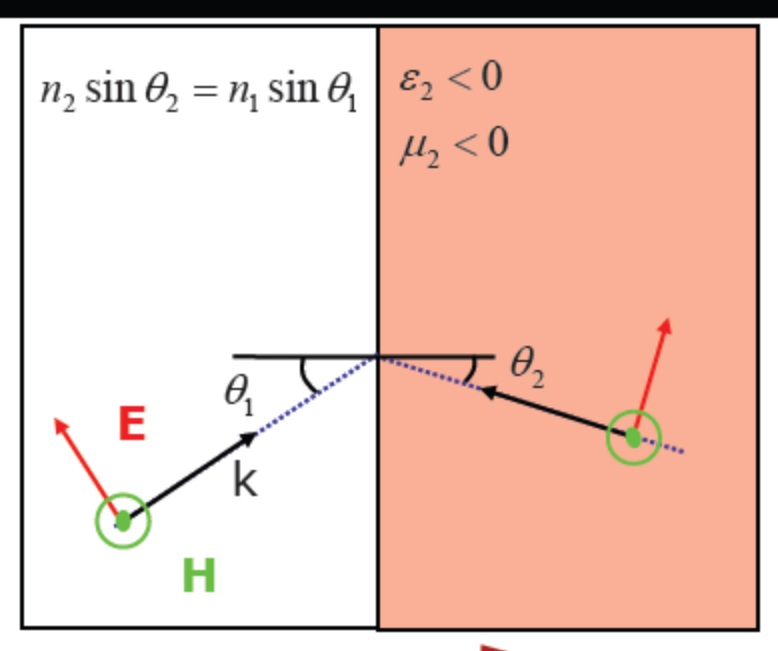
$$n^2 - ex.$$
 (3)

If we do not take losses into account and regard n, ϵ , and μ as real numbers, it can be seen from (2) and (3) that a simultaneous change of the signs of ϵ and μ has no effect on these relations.

This situation can be interpreted in various ways. First, we may admit that the properties of a substance are actually not affected by a simultaneous change of the signs of e and μ . Second, it might be that for ϵ and μ to be simultaneously negative contradicts some fundamental laws of nature, and therefore no substance with $\epsilon \le 0$ and $\mu \le 0$ can exist. Finally, it could be admitted that substances with negative 4 and \$\mu\$ have some properties different from those of substances with positive c and \u03c4. As we shall see in what follows, the third case is the one that is realized. It must be emphasized that there has not so far been any experiment in which a substance with $\epsilon < \sigma$ and μ < 0 could be observed. We can, however, at once give a number of arguments as to where and how one should look for such substances. Since in our opinion the electrodynamics of substances with $\epsilon \le 0$ and μ < 0 is undoubtedly of interest, independently of our.
</p> now having such substances available, we shall at first consider the matter purely formally. Thereafter in the second part of this article we shall consider questions connected with the physical realization of substances with $\epsilon < 0$ and $\mu < 0$.

Refraction in Right and Left-Handed Media





Energy propagation

$$\mathbf{S} = \frac{c}{4\pi} [\mathbf{E}\mathbf{H}]$$

Energy propagation

$$\begin{cases} k \times H = -\omega \varepsilon_0 \varepsilon E \\ \vec{k} \times \vec{E} = \omega \mu_0 \mu \vec{H} \end{cases}$$

$$n = \pm \sqrt{\varepsilon \mu}$$

PIM
$$\longrightarrow S = ExF$$

- Inverse Doppler effect
- Inverse Snell law
- Inverse Cerenkov effect
- Inverse Light pressure
- ...

Experimental realization

The existence of artificial 'atoms' yielding μ < 0 makes it possible to construct a material with ϵ <0 and μ <0:

VOLUME 84, NUMBER 18

PHYSICAL REVIEW LETTERS

1 MAY 2000

Composite Medium with Simultaneously Negative Permeability and Permittivity

D. R. Smith,* Willie J. Padilla, D. C. Vier, S. C. Nemat-Nasser, and S. Schultz

Department of Physics, University of California, San Diego, 9500 Gilman Drive, La Jolla, California 92093-0319

(Received 2 December 1999)

We demonstrate a composite medium, based on a periodic array of interspaced conducting nonmagnetic split ring resonators and continuous wires, that exhibits a frequency region in the microwave regime with simultaneously negative values of effective permeability $\mu_{\rm eff}(\omega)$ and permittivity $s_{\rm eff}(\omega)$. This structure forms a "left-handed" medium, for which it has been predicted that such phenomena as the Doppler effect, Cherenkov radiation, and even Snell's law are inverted. It is now possible through microwave experiments to test for these effects using this new metamaterial.

Illi Ext. If Winiresonant

≥ Veff Lessnert

Measurements and calculations

Measured magnetic resonance of 2D split ring structure

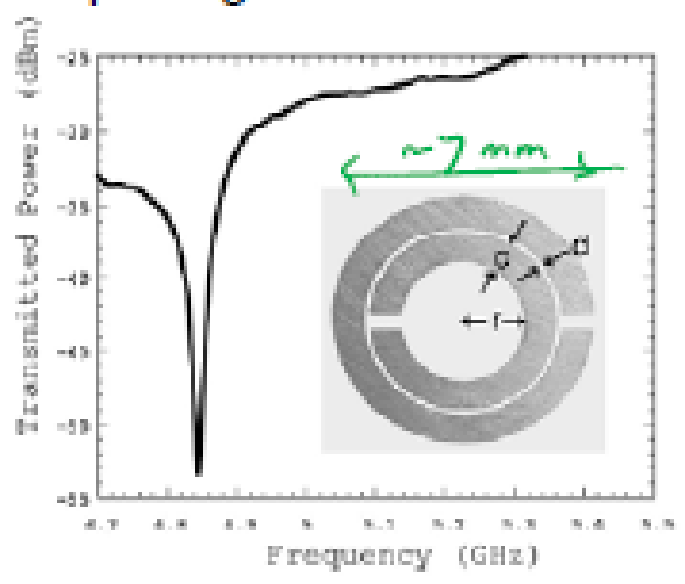
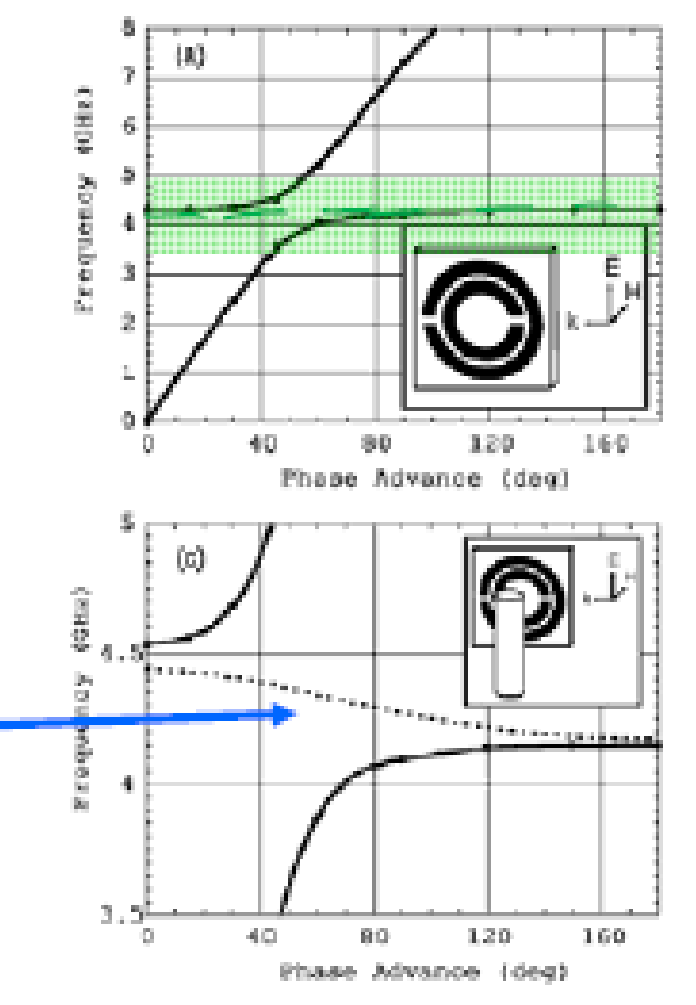


FIG. 1. Resonance curve of an actual copper split ring resonance (SRR). c = 0.8 mm, d = 0.2 mm, and r = 1.5 mm. The SRR has its resonance at about 4.845 GHz, and the quality factor has been measured to be $Q = f_0/\Delta f_{MB} > 600$, consistent with numerical signalations.

When were are added symmetrically between the split rings, for the H_{\parallel} case a passband occurs within the previously forbidden band of the split ring dispersion curves of Fig. 2(a). That this passband [the dashed line in Fig. 2(c)] occurs within a previously forbidden region indicates that the negative $v_{\rm eff}(\omega)$ for this region has combined with the negative $\mu_{\rm eff}(\omega)$ to allow propagation, as predicted. Calculated dispersion curves for rings only, and rings + rods (providing negative ε for certain λ)



Calculations show that this anisotropic structure exhibits negative group velocity

Transmission experiment

Predictions confirmed by measurement!

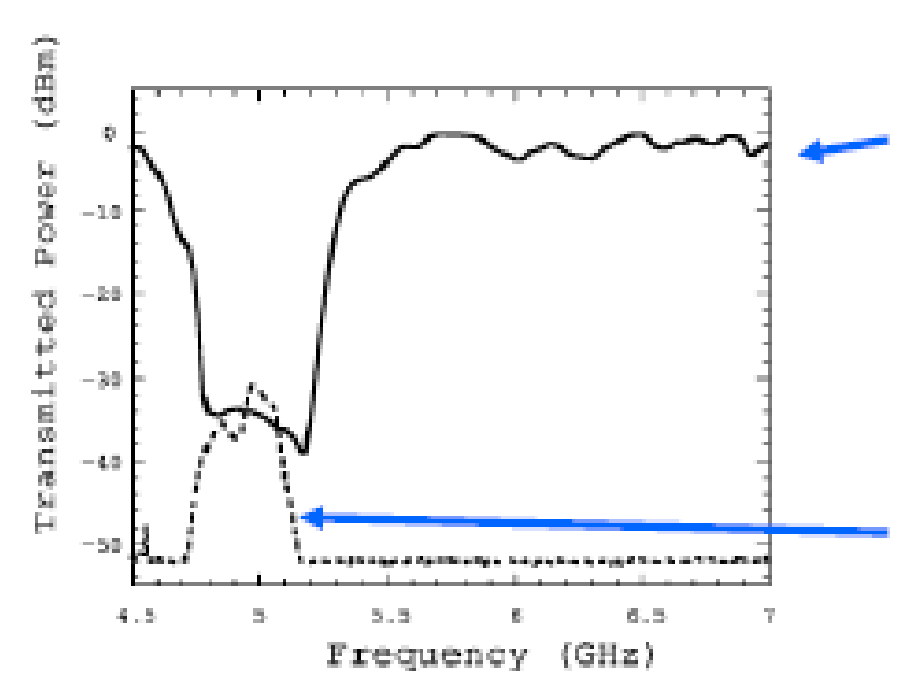


FIG. 3. A transmission experiment for the case of $H_{\rm H}$. The upper curve (solid line) is that of the SRR array with lattice parameter a=8.0 mm. By adding wires uniformly between split rings, a passband occurs where μ and e are both negative (dashed curve). The transmitted power of the wires alone is coincident with that of the instrumental noise floor (-52 dB).

Split rings only:

EM wave transmission impeded at frequencies where $\mu < 0$

Adding parallel wires to unit cell, ε<0 obtained. In this case, transmission is enabled in a small frequency band where ε<0 and μ<0

Next step: demonstrate negative refraction?

Negative refraction observed



In 2001, three years after Pendry's split ring proposal and close to 40 years after Veselago's first paper on negative refraction:

Experimental Verification of a Negative Index of Refraction

R. A. Shelby, D. R. Smith, S. Schultz

We present experimental scattering data at microwave frequencies on a structured metamaterial that exhibits a frequency band where the effective index of refraction (n) is negative. The material consists of a two-dimensional array of repeated unit cells of copper strips and split ring resonators on interlocking strips of standard circuit board material. By measuring the scattering angle of the transmitted beam through a prism fabricated from this material, we determine the effective n, appropriate to Snell's law. These experiments directly confirm the predictions of Maxwell's equations that n is given by the negative square root of $e \cdot \mu$ for the frequencies where both the permittivity (e) and the permeability (μ) are negative. Configurations of geometrical optical designs are now possible that could not be realized by positive index materials.

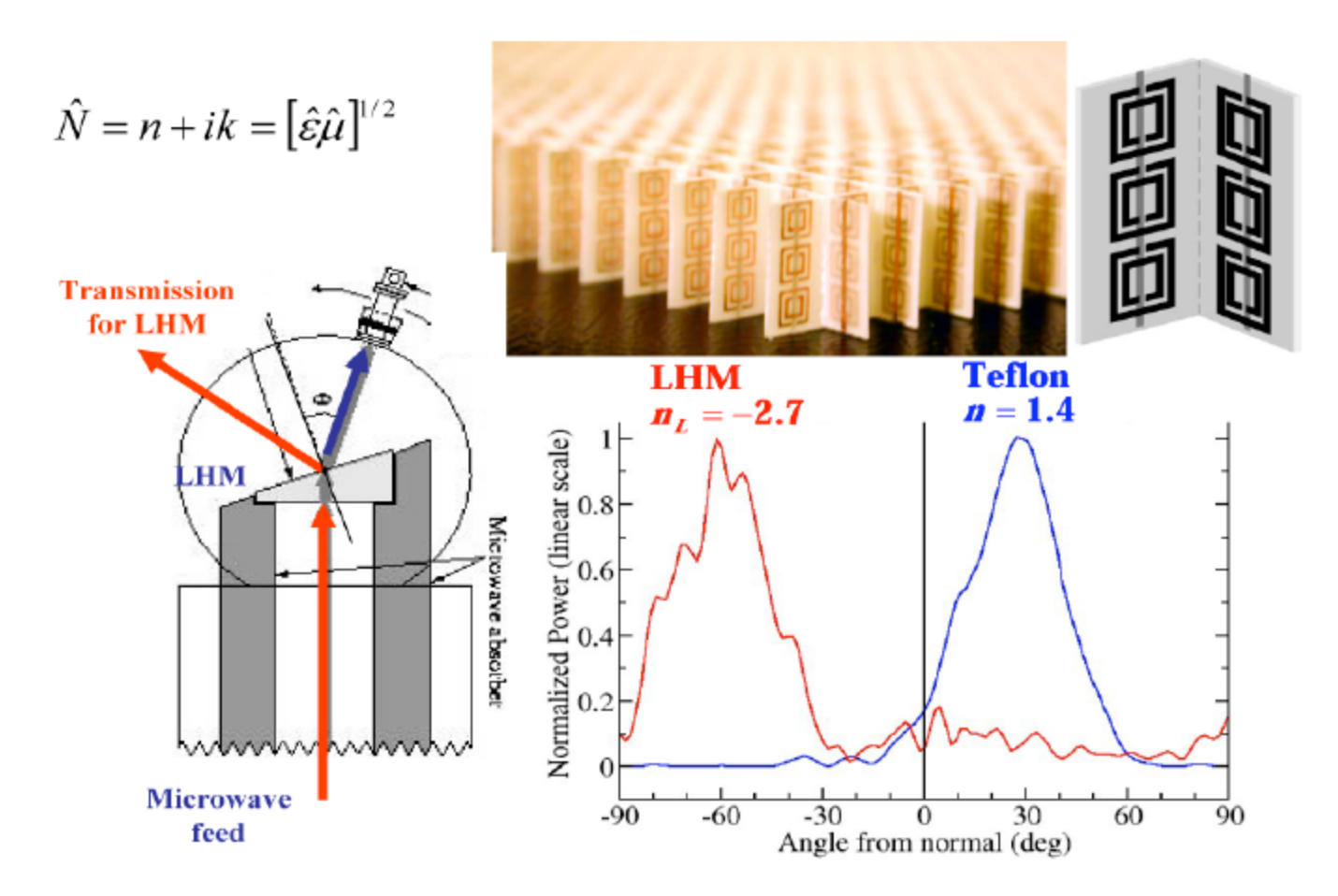
www.sciencemag.org SCIENCE VOL 292 6 APRIL 2001



Fig. 1. Photograph of the lefthanded metamaterial. (LHM) sample. The LHM sample consists of square copper split ring resonators and copper wire strips on fiber glass circuit board material. The rings and wires are on opposite sides of the boards, and the boards have been cut and assembled into an interlocking lattice.

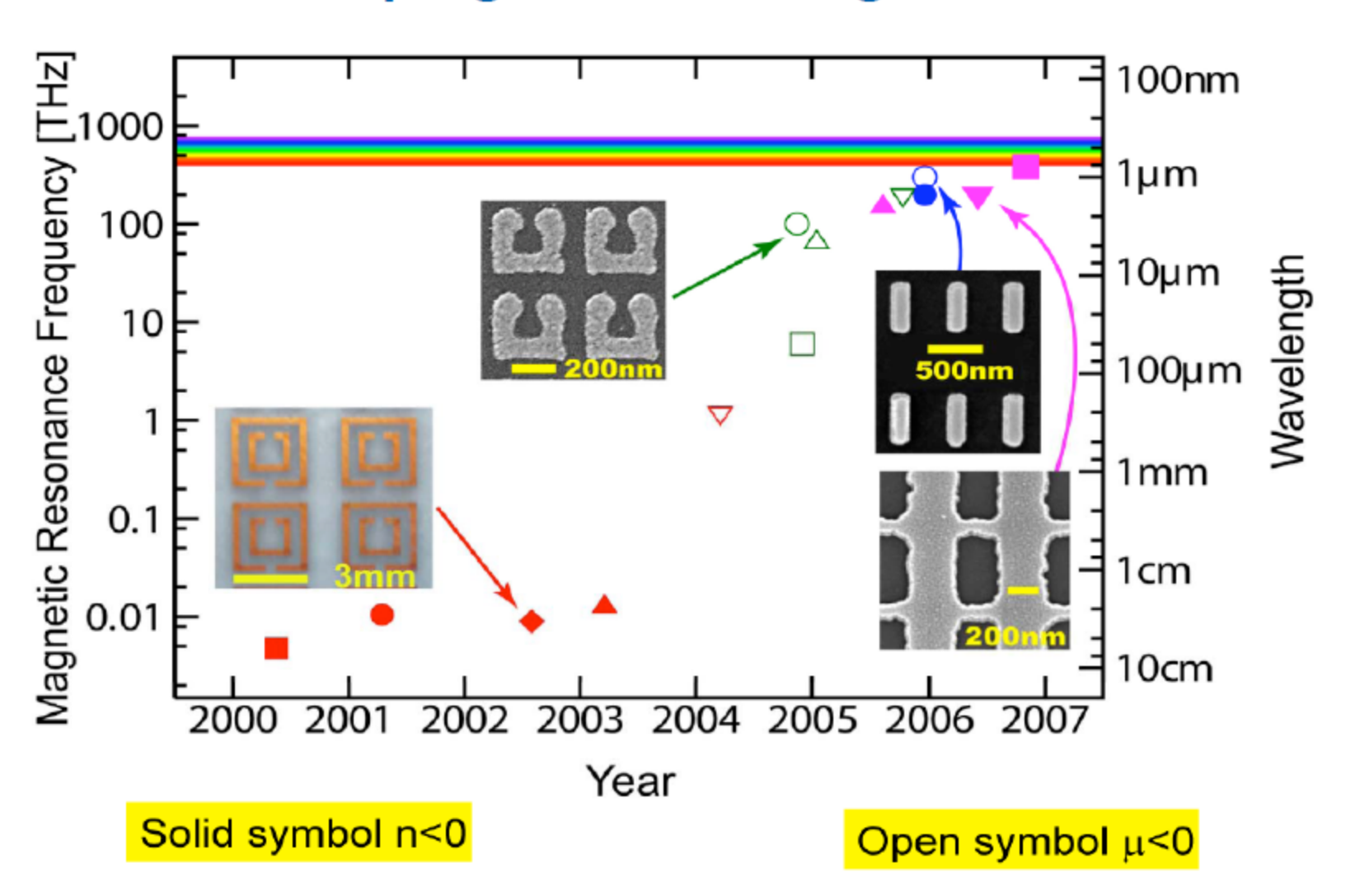
Experiments at microwave frequencies Approximately 2D isotropic response (2 orientations of rings)

Refraction in negative index media (NIM)



R.A. Shelby, D.R. Smith, S. Schultz, Science 292, 77 (2001)

The progress of scaling materials



Vol 455 18 September 2008 doi:10.1038/nat

LETTERS

Three-dimensional optical metamaterial with a negative refractive index

 $\label{eq:lambda} {\sf Jason\ Valentine}^{1*}, {\sf Shuang\ Zhang}^{1*}, {\sf Thomas\ Zentgraf}^{1*}, {\sf Erick\ Ulin-Avila}^1, {\sf Dentcho\ A.\ Genov}^1, {\sf Guy\ Barta\ \&\ Xiang\ Zhang}^{1}}$

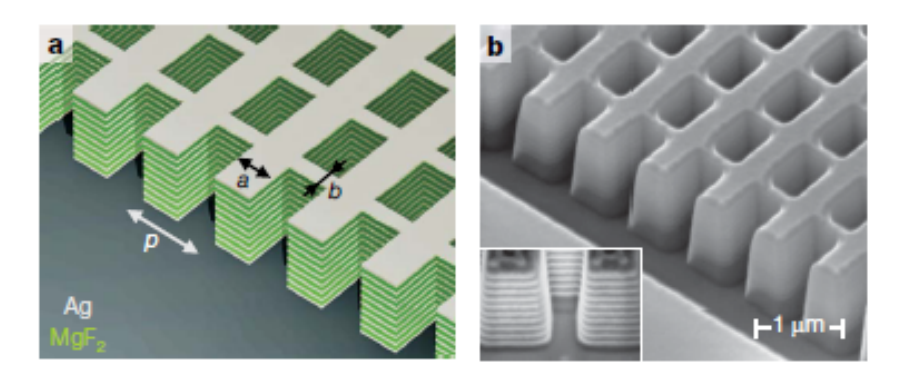
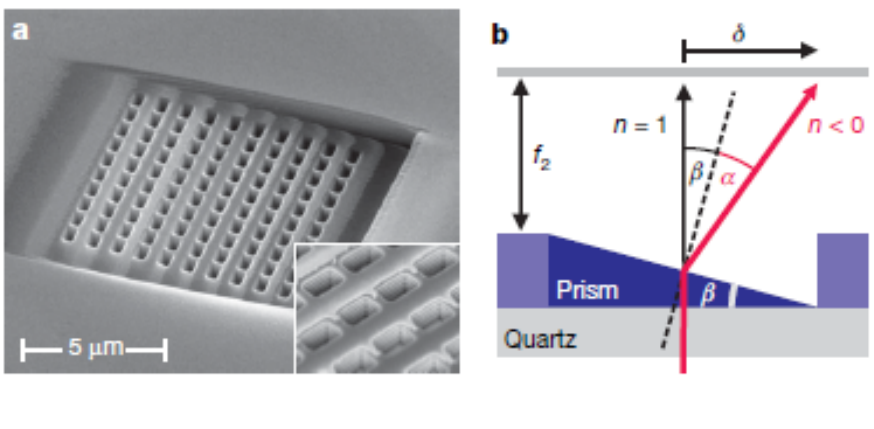


Figure 1 | Diagram and SEM image of fabricated fishnet structure. a, Diagram of the 21-layer fishnet structure with a unit cell of $p=860\,\mathrm{nm}$, $a=565\,\mathrm{nm}$ and $b=265\,\mathrm{nm}$. b, SEM image of the 21-layer fishnet structure with the side etched, showing the cross-section. The structure consists of alternating layers of 30 nm silver (Ag) and 50 nm magnesium fluoride (MgF₂), and the dimensions of the structure correspond to the diagram in a. The inset shows a cross-section of the pattern taken at a 45° angle. The sidewall angle is 43° and was found to have a minor effect on the transmittance curve according to simulation.



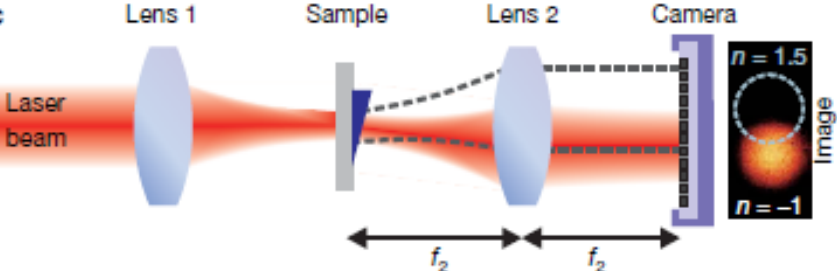


Figure 2 | SEM image of NIM prism and schematics of experimental setup. a, SEM image of the fabricated 3D fishnet NIM prism. The unit cell size is identical to that shown in Fig. 1a. The inset shows a magnified view with the film layers visible in each hole. b, Geometry diagram of the angle measurement; δ corresponds to the position difference of the beam passing through a window in the multilayer structure (n=1) and prism sample. By measuring δ , the absolute angle of refraction α can be obtained. c, Experimental setup for the beam refraction measurement. The focal length of lens 1 is 50 mm and that of lens 2 is $f_2=40$ mm. Lens 2 is placed in a 2f configuration, resulting in the Fourier image at the camera position.

Super-Resolution: Amplification of evanescent waves

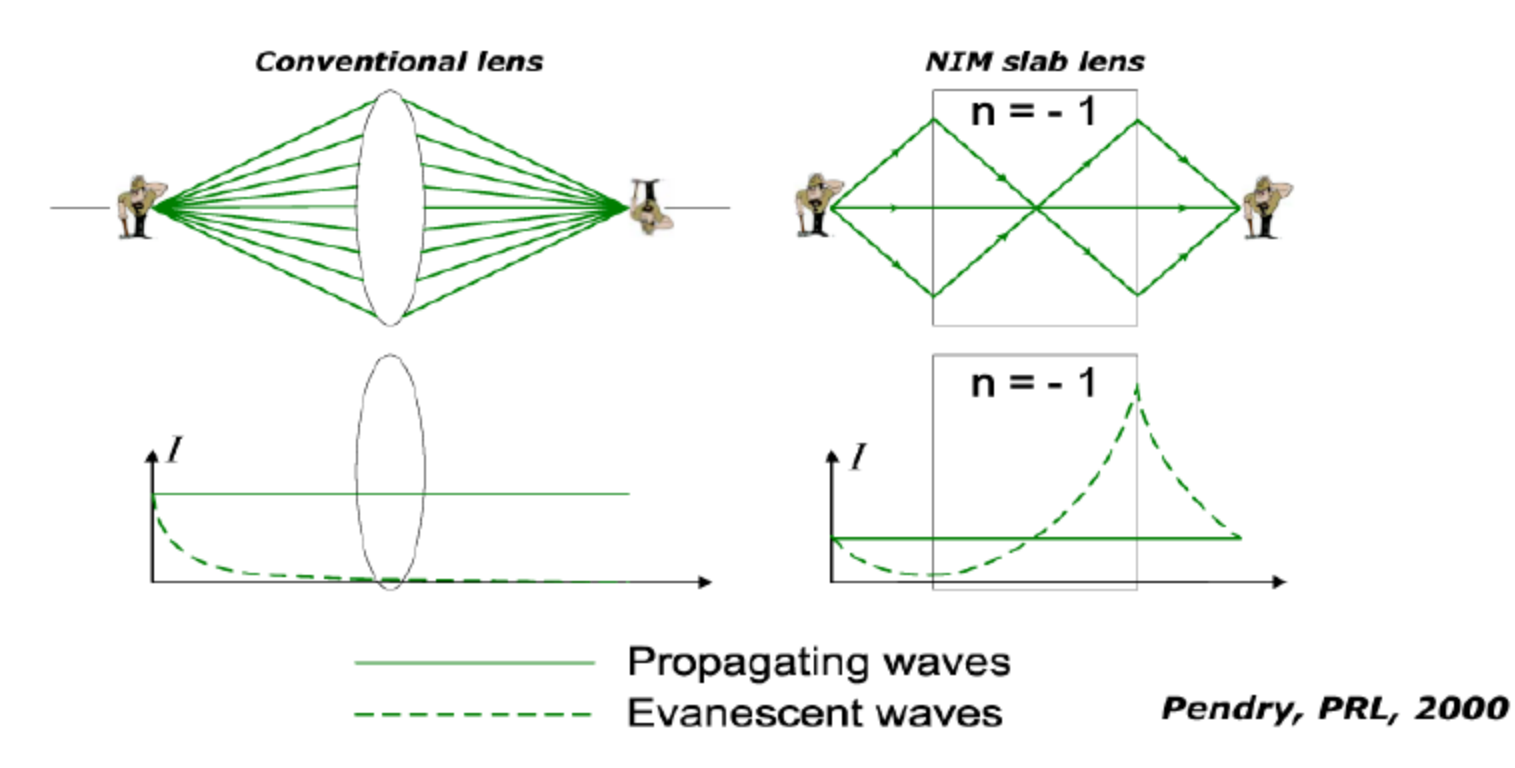
Waves scattered by an object have all the Fourier components. The propagating waves are limited to: $k_r = \sqrt{k_x^2 + k_y^2} < k_0$

 $k_z = \sqrt{k_0^2 - k_x^2 - k_y^2}$

$$k_{t} = \sqrt{k_{x}^{2} + k_{y}^{2}} < k_{0}$$

$$\lambda_i = 2\pi/k_i < \Delta, \quad \Delta < \lambda \Rightarrow \quad k_i = \sqrt{k_x^2 + k_y^2} > k_0, \quad k_z^2 < 0$$

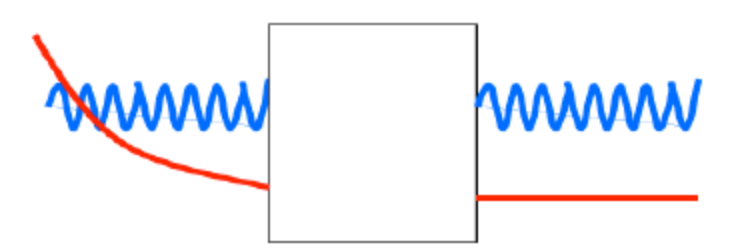
To resolve features Δ , we must have $\lambda_{r} = \sqrt{k_{x}^{*} + k_{y}^{*}} < k_{0}$ The evanescent waves are "re-grown" in a NIM slab and fully recovered at the image plane



Optical super- and hyper-lens

Ordinary Lens:

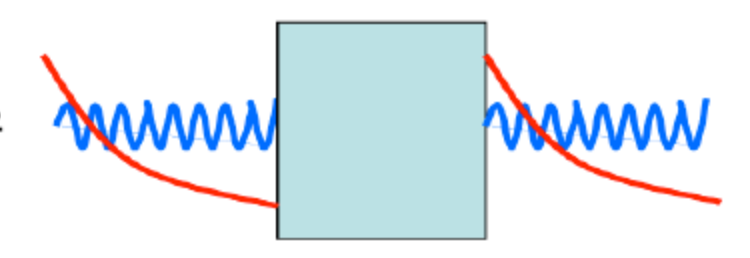
evanescent field lost



Super Lens:

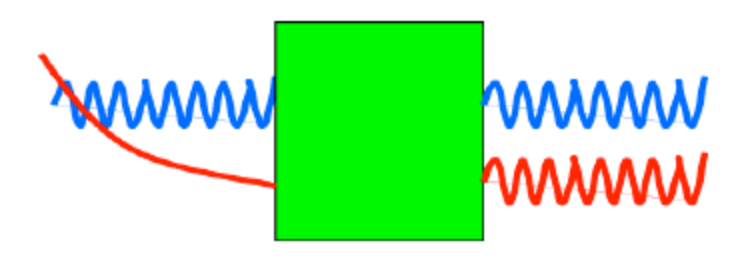
evanescent field enhanced but decays away from the lens

- * LIMITED TO NEAR FIELD
- * EXPONENTIALLY SENSITIVE TO DISORDER, LOSSES,...

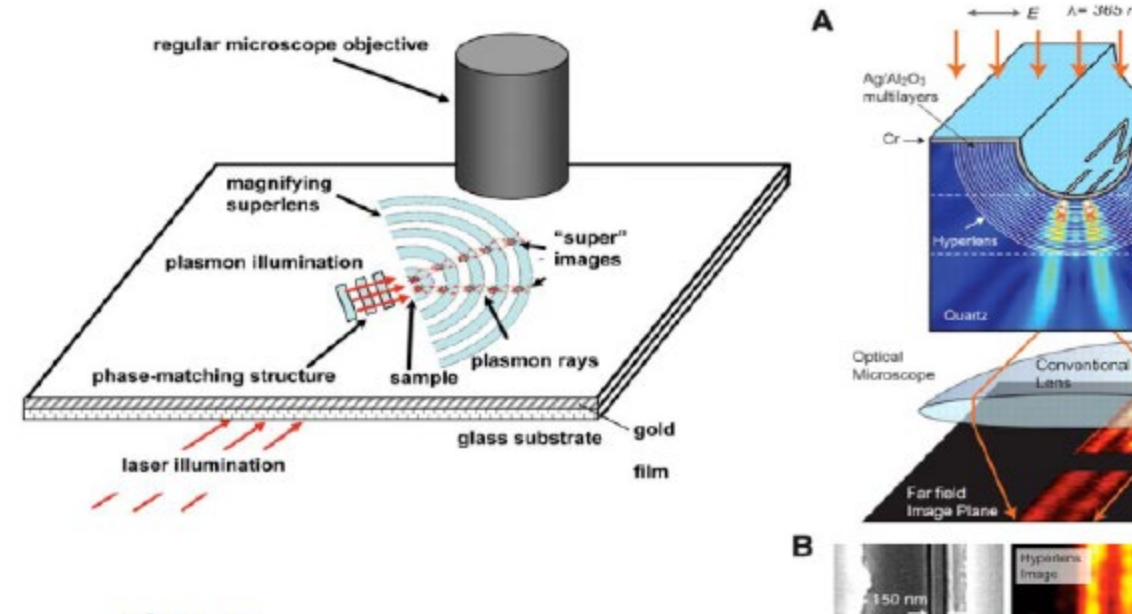


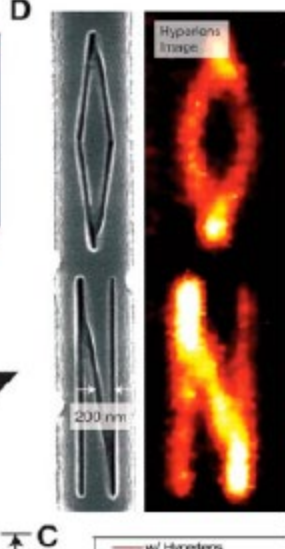
Hyper Lens:

evanescent field converted to propagating waves (that do not mix with the others)



Optical hyper-lens

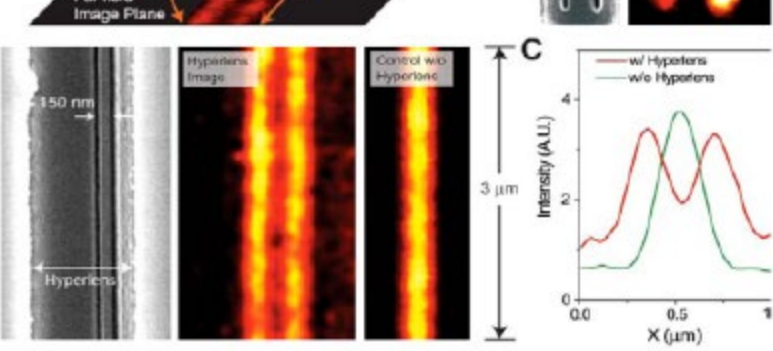




Theory:

Jacob, Narimanov, OL, 2006 Salandrino, Engehta, PRB, 2006 Experiments:

Z. Liu et al., Science, 2007 Smolyaninov et al., Science, 2007

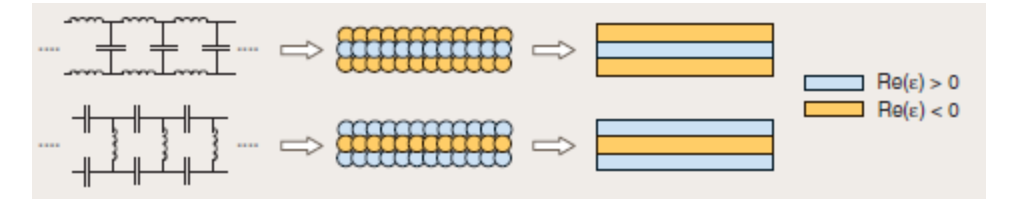


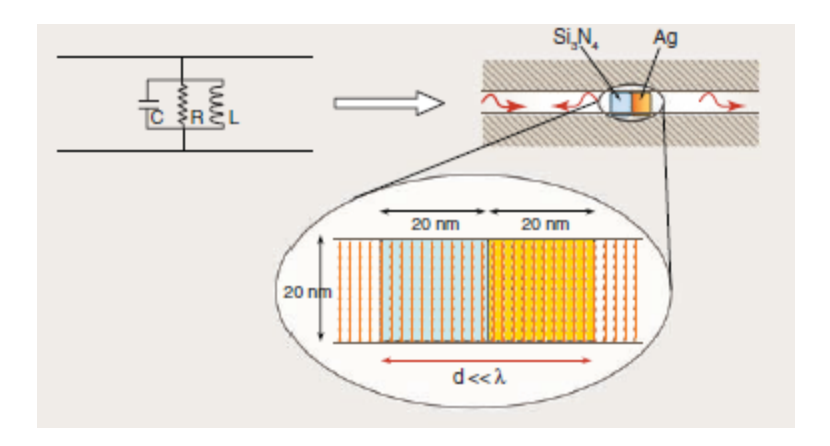
Hypertens Image Plane

REVIEW

Circuits with Light at Nanoscales: Optical Nanocircuits Inspired by Metamaterials

Nader Engheta





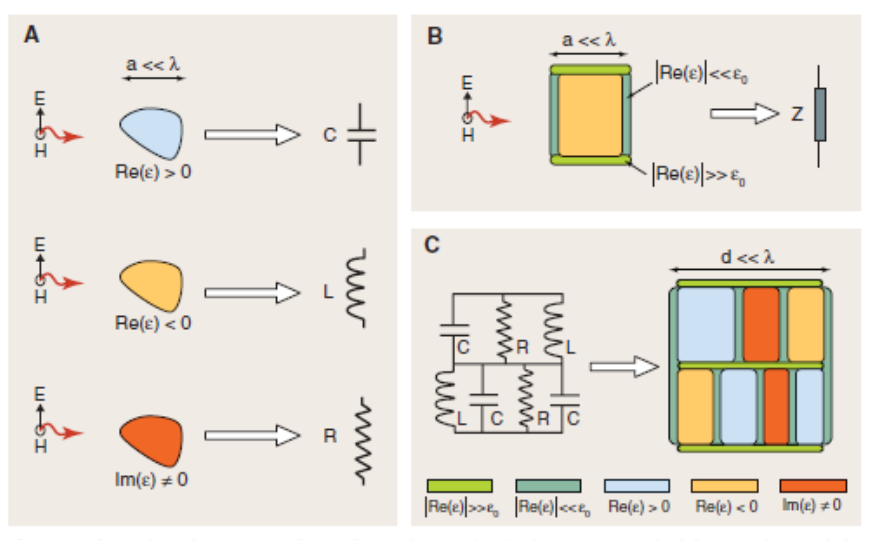


Fig. 1. Subwavelength nanoparticles as lumped nanocircuit elements at optical frequencies, and the collections of such nanoparticles. (**A**) A nanoparticle, with subwavelength size, when illuminated by a monochromatic optical signal, can effectively play the role of a lumped optical circuit element, depending on the permittivity of its material (2). (**B**) An optical nanomodule, formed by a material nanoparticle with subwavelength size, covered on its sides by layers of material with a very low real part of relative permittivity and on its two ends by layers of material with a very high real part of relative permittivity. This may perform as an insulated, lumped optical nanoelement with two connecting terminals. (**C**) Illustration of the concept of mn-circuits, several lumped optical nanomodules of (B), arranged next to each other, with a subwavelength dimension. When this mn-circuit is excited by an optical signal, the optical electric fields and displacement currents in these elements are tailored and patterned such that this collection of particles may behave approximately as the circuit shown on the left in a specific frequency band.